Table 1. Summary of the Literature on Disease Modeling Using Patient-Specific iPSCs

Disease	Gene mutation	Cell type	Cellular phenotype	Refs.
AD	PS1 mutations	Neurons	Increase in Aβ secretion and rescued by γ-secretase inhibitors	44)
PD	LRRK2 mutations	Neurons-dopaminergic	Degeneration due to increased oxidative-stress	45)
CPVT	RYR2 mutations	Cardiomyocytes	Abnormal dynamism in Ca handling and treatment with several drugs rescues the phenotype	46)
DCM	TNNT2 mutations	Cardiomyocytes	Altered regulation of Ca emphasized by β adrenergic agonist and rescued by β blocker	47)
FH	LDL receptor mutations	Hepatocytes	Impaired ability to incorporate LDL	48)
CML	BCR-ABL	iPSCs, Hematopoietic cells	Imatinib resistant in iPSCs and immature Hematopoietic cells	49)
MD (+DM)	mtDNA A3243G mutation	iPSCs, EBs	Variety of degree of mutation heteroplasmy in each iPSC clones	50)
DS (+AD)	Trisomy 21	Neurons-cortical	Secretion of the pathogenic peptide fragment amyloid-β42	51)
DKC	DKC1, TERT, TCAB1 mutation	iPSCs	Progressive telomere shortening and loss of self-renewal of iPSCs	52), 53)
RP	RP1, RP9, PRPH2, RHO mutations	Rod photoreceptor cells	Decreased numbers of differentiated rod cells and expression of cellular stress markers	54)
GD	GCase mutations	Neurons-dopaminergic	Lysosomal protein degradation, causes accumulation of α-synuclein	55)

AD: Alzheimer's Disease, PD: Parkinson's Disease, CPVT: Catecholaminergic Polymorphic Ventricular Tachycardia, DCM: Dilated Cardiomyopathy, FH: Familial Hypercholesterolemia, CML: Clonic Myeloid Leukemia, MD: Mitochondrial Disease, DM: Diabetes Mellitus, DS: Down Syndrome, DKC: Dyskeratosis Congenita, RP: Retinitis Pigmentosa, GD Gaucher Disease.

family members partly share genetic information including single-nucleotide polymorphisms, and this could affect disease phenotype. A recent study has demonstrated that ideal control iPSCs can be obtained by mutated gene correction using a targeting strategy.[29,30] Even though it cannot be applied in every disease model, further analysis using isogenic-control iPSCs may be the answer to this problem.

Differentiation into Disease Relevant-Cells iPSCs can give rise to a wide variety of cell types present in the three germ layers. In most cases, differentiation methods for iPSCs are applied with some modification from the methods established in embryonic stem cells, which are similar to the regulatory mechanisms of normal early development.[8,9] To establish methods for *in vitro* differentiation from pluripotent stem cells, various screening methods for essential signaling molecules in normal development have been performed.[31]

Among several iPSC lines, the variation in differentiation propensity into specific cell types is well known.[32,33] Therefore the cell type of each iPSC generated should be confirmed before selecting the optimal cell line that can most efficiently differentiate into the cells of interest. A recent study has shown that iPSCs maintain epigenetic memories originally belonging to somatic cells, and this epigenetic status can regulate the characteristics of iPSCs, especially their differentiation propensity.[34–36] Therefore it is important to confirm which cells are the best source for iPSCs to obtain stable, disease-relevant cells.

To investigate more sophisticated experimental conditions similar to the physiologic environment, further improvements are required. First, it is necessary to establish a procedure to purify the cells from aggregations of iPSC-derived miscellaneous cells.[37,38] In addition, it would be ideal to be able to differentiate iPSCs into all constitutive cell types of an organ. In other words, to create organs *in vitro*, not only a single specific cell type but also other cell types such as endothelial cells, fibroblasts, and peripheral neural cells are needed. Furthermore, there are various subpopulations among cardiomyocytes such as atrial-, nodal- and ventricular-type cardiomyocytes, although at present there is no method to obtain each specific cell type.[39] These are crucial limitations on the reliability of results of the novel iPSC assay. In addition, iPSC-derived cells retain the original fetal-like characteristics, and it remains unclear how these cells can be appropriately matured.[40] Still another unresolved issue is the best time in the developmental stage of patient-specific iPSC-derived cells to analyze cellular function in terms of disease properties.

A recent advance in reprogramming to change the cellular fate is direct conversion, which allows terminally differentiated cells to be transformed into other functional cells of different lineages without passing through the pluripotent state.[41,42] In this method, mature target cells can be obtained within a shorter period, and disease modeling using this direct conversion technique has also been reported.[43] However, in spite of lower induction efficiency and the lack of a method established for all cell lineages, iPSCs seem to be a suitable cell source for disease modeling. The infinite self-renewability of iPSCs allows repetitive, reproducible analysis of the disease cells of interest.

Disease Modeling Using Patient-Specific iPSCs To date, several patient-specific iPSC lines have been generated from patients with a wide variety of mainly monogenetic, early-onset diseases such as neurologic disorders,[44,45] heart disease,[46,47] metabolic disease,[48] hematologic disorders,[49] mitochondrial disease,[50] chromosomal abnormalities,[51] telomere disease,[52,53] sensory organ disorder,[54] and storage disease.[55] The current list of studies of disease modeling using patient-specific iPSCs is shown in Table 1. While findings on patient-specific iPSCs have accumulated, analysis becomes more complicated in polygenic, sporadic, late-onset disease.[12,56,57] The next steps that will deliver useful clinical information resulting from patient-specific iPSC technology will result from collaborations between academic research groups and

pharmaceutical companies, which are expected develop novel therapeutic compounds and clarify possible sife effects through advanced high-throughput screening systems using patient-specific iPSC-derived cells.

3. CARDIOVASCULAR DISEASE MODELING USING iPSCs

Functional Characteristics of iPSC-Derived Cardiomyocytes On the premise that the study of human cardiovascular disease modeling will be initiated using patient-specific iPSCs, it is necessary to confirm that the characteristics of human iPSC-derived cardiomyocytes are physiologically analogous to human cardiomyocytes *in vivo*. Previous molecular biological and physiologic studies revealed that iPSC-derived cardiomyocytes have normal cardiomyocyte functional properties.[58,59] iPSC-derived cardiomyocytes have a striated muscle structure identical to that of normal functional cardiomyocytes and express cardiac-specific proteins, as confirmed in molecular biological assays such as immunocytochemistry and reverse-transcriptase polymerase chain reaction (PCR). Based on the waveform of the action potential, iPSC-derived cardiomyocytes can be divided into three subpopulations: atrial, nodal, and ventricular cells. Moreover, the contraction of iPSC-derived cardiomyocytes is regulated by physiologic intracellular signaling including excitation-contraction coupling,[60] and those cardiomyocytes express typical ion channels with the expected functional responses to several ion channel blockers.[61] All these findings indicate the validity of studies that will lead to the analysis of cardiovascular disease using patient-specific iPSC-derived cardiomyocytes.

Modeling LQTS Type 1 Some groups thought that LQTS would be a suitable disease for modeling using iPSCs because of the promising reproducibility of disease phenotypes in iPSC-derived cardiomyocytes.[13,62–67] Moretti *et al.* first showed that patient-specific iPSC-derived cardiomyocytes could recapitulate the disease phenotype in congenital LQTS.[62] They generated iPSCs from two patients with LQTS type 1, who had autosomal-dominant inheritance of a G569A missense mutation in the *KCNQ1* gene encoding the IKs current which was previously shown to be relevant to LQTS onset by functional analysis of the mutated gene.[68]

Individual cardiomyocytes derived from LQTS type 1 patient-specific iPSCs (LQTS1-iPSC-CMs) showed prolonged action potentials using whole-cell patch clamping compared with cardiomyocytes from healthy control donors who were unrelated to the patients. Moreover, LQTS1-iPSC-CMs exhibited increased susceptibility to catecholamine-induced tachyarrhythmia, which is one of the most important clinical features of the syndrome.[69] Even though that study was recognized as an important work first confirming the great potential of patient-specific iPSCs, we thought that there was room for expansion of the scope. In not only that study but also in other reports of LQTS disease modeling using iPSCs, patients who had mutated channel profiles characterized by conventional experimental methods were selected. In reality, many patients have unknown mutations that give no specific information on their disease phenotype. To address whether iPSC technology could be used to characterize the disease phenotype with a novel mutated gene, we selected LQTS patients with no family history or previous disease characterization.[13]

We generated iPSCs from a 13-year-old boy who was a sporadic LQTS patient. He had survived cardiopulmonary arrest due to ventricular fibrillation, and his subtype of LQTS could not be diagnosed using standard clinical tests.[70,71] Two healthy volunteers served as controls who donated iPSCs that had differentiated into cardiomyocytes. Our patient had a novel heterozygous mutation located in the *KCNQ1* gene, 1893delC, identified by genotyping of his blood sample.[72] Electrophysiologic function was measured using a multielectrode array system,[73] which showed that the duration of the field potential was markedly prolonged in LQTS-iPSCs-CMs as compared with cardiomyocytes derived from controls, which suggested that LQTS-iPSC-CMs maintained the patient's characteristics and could be successfully reproduced in this assay system.

Next we tried to confirm the responsible channel for the disease phenotype by precise evaluation of several drug responses. We clarified that the IKs channel was functionally impaired and that the IKr channel could compensate for this effect in LQTS-iPSC-CMs with the administration of several potassium current blockers. In general, the IKr and IKs channels work in a complementary fashion in the repolarization of cardiomyocytes, which is known as the repolarization reserve,[74] and we confirmed that this mechanism regulated the balance of the potassium current in LQTS-iPSC-CMs. Arrhythmogenic events in LQTS-iPSC-CMs caused by adrenergic stimulation also suggested that the patient's IK channel was significantly attenuated.[70,71] These findings strongly suggested that cardiomyocytes in the patient's IKs channel were functionally impaired and that the precise diagnosis was LQTS type 1.[75] To confirm the dominant-negative role of the *KCNQ1* 1893delC mutation in IKs channel function, we performed electrophysiologic and histochemical analyses in iPSC-derived cardiomyocytes and found that *KCNQ1* 1893delC has a dominant-negative effect *via* a trafficking deficiency.

Importantly, our study demonstrated that iPSCs could be useful to characterize the electrophysiologic cellular phenotype of a patient with a novel mutation. We performed functional analysis of the novel mutation using patient-specific iPSCs, which may support the diagnosis of LQTS type 1. Moreover, this system allowed us to perform several drug administration tests on LQTS-iPSC-CMs, which would be extremely risky to such a patient in clinical practice.[76] Therefore patient-specific iPSC technology can be used for drug evaluation and monitoring. At the same time, we were able to clarify the underlying molecular mechanism of the disease phenotype using this assay system.

4. CONCLUSION

Although iPSC technology is an attractive tool for analyzing human genetic diseases, it is clear that technological innovation remains necessary for the utilization of iPSCs in routine medical practice. Disease modeling using patient-specific iPSCs is a novel procedure for analyzing disease. It enables a direct, repetitive approach to diseased cells and has great potential to elucidate novel disease pathogenesis and develop new therapeutic compounds. However, in terms of the effort, cost, and time required in current studies using iPSCs, routine clinical usage is not yet feasible.[77] In addition, improvement of the quality of iPSCs and iPSC-derived cells is required

to make disease models using iPSCs more faithful. Some problems such as genetic mutations during reprogramming, incomplete epigenetic reprogramming, and undesired gene expression should also be controlled and standardized. More sophisticated differentiation, maturation, and purification protocols will be indispensable to create physiologic cellular conditions that reflect the actual disease phenotype.

In conclusion, steady progress is being made in iPSC technology to overcome the hurdles, and disease modeling using iPSCs appears a likely technique for the future. Recent and future innovations in the technique hold out the promise of patient-derived iPSC technology to achieve personalized medicine in the clinical setting.

REFERENCES

1) Takahashi K, Tanabe K, Ohnuki M, Narita M, Ichisaka T, Tomoda K, Yamanaka S. Induction of pluripotent stem cells from adult human fibroblasts by defined factors. *Cell*, **131**, 861–872 (2007).
2) Yu J, Vodyanik MA, Smuga-Otto K, Antosiewicz-Bourget J, Frane JL, Tian S, Nie J, Jonsdottir GA, Ruotti V, Stewart R, Slukvin II, Thomson JA. Induced pluripotent stem cell lines derived from human somatic cells. *Science*, **318**, 1917–1920 (2007).
3) Yu J, Hu K, Smuga-Otto K, Tian S, Stewart R, Slukvin II, Thomson JA. Human induced pluripotent stem cells free of vector and transgene sequences. *Science*, **324**, 797–801 (2009).
4) Kim D, Kim C-H, Moon J-I, Chung YG, Chang MY, Han BS, Ko S, Yang E, Cha KY, Lanza R, Kim KS. Generation of human induced pluripotent stem cells by direct delivery of reprogramming proteins. *Cell Stem Cell*, **4**, 472–476 (2009).
5) Ban H, Nishishita N, Fusaki N, Tabata T, Saeki K, Shikamura M, Takada N, Inoue M, Hasegawa M, Kawamata S, Nishikawa S. Efficient generation of transgene-free human induced pluripotent stem cells (iPSCs) by temperature-sensitive Sendai virus vectors. *Proc. Natl. Acad. Sci. U.S.A.*, **108**, 14234–14239 (2011).
6) Warren L, Manos PD, Ahfeldt T, Loh YH, Li H, Lau F, Ebina W, Mandal PK, Smith ZD, Meissner A, Daley GQ, Brack AS, Collins JJ, Cowan C, Schlaeger TM, Rossi DJ. Highly efficient reprogramming to pluripotency and directed differentiation of human cells with synthetic modified mRNA. *Cell Stem Cell*, **7**, 618–630 (2010).
7) Miyoshi N, Ishii H, Nagano H, Haraguchi N, Dewi DL, Kano Y, Nishikawa S, Tanemura M, Mimori K, Tanaka F, Saito T, Nishimura J, Takemasa I, Mizushima T, Ikeda M, Yamamoto H, Sekimoto M, Doki Y, Mori M. Reprogramming of mouse and human cells to pluripotency using mature microRNAs. *Cell Stem Cell*, **8**, 633–638 (2011).
8) Murry CE, Keller G. Differentiation of embryonic stem cells to clinically relevant populations: lessons from embryonic development. *Cell*, **132**, 661–680 (2008).
9) Irion S, Nostro MC, Kattman SJ, Keller GM. Directed differentiation of pluripotent stem cells: from developmental biology to therapeutic applications. *Cold Spring Harb. Symp. Quant. Biol.*, **73**, 101–110 (2008).
10) Byrne JA. Generation of isogenic pluripotent stem cells. *Hum. Mol. Genet.*, **17** (R1), R37–R41 (2008).
11) Ebert AD, Yu J, Rose FF Jr, Mattis VB, Lorson CL, Thomson JA, Svendsen CN. Induced pluripotent stem cells from a spinal muscular atrophy patient. *Nature*, **457**, 277–280 (2009).
12) Brennand KJ, Simone A, Jou J, Gelboin-Burkhart C, Tran N, Sangar S, Li Y, Mu Y, Chen G, Yu D, McCarthy S, Sebat J, Gage FH. Modelling schizophrenia using human induced pluripotent stem cells. *Nature*, **473**, 221–225 (2011).
13) Egashira T, Yuasa S, Suzuki T, Aizawa Y, Yamakawa H, Matsuhashi T, Ohno Y, Tohyama S, Okata S, Seki T, Kuroda Y, Yae K, Hashimoto H, Tanaka T, Hattori F, Sato T, Miyoshi S, Takatsuki S, Murata M, Kurokawa J, Furukawa T, Makita N, Aiba T, Shimizu W, Horie M, Kamiya K, Kodama I, Ogawa S, Fukuda K. Disease characterization using LQTS-specific induced pluripotent stem cells. *Cardiovasc. Res.*, **95**, 419–429 (2012).
14) Osafune K, Caron L, Borowiak M, Martinez RJ, Fitz-Gerald CS, Sato Y, Cowan CA, Chien KR, Melton DA. Marked differences in differentiation propensity among human embryonic stem cell lines. *Nat. Biotechnol.*, **26**, 313–315 (2008).
15) Dimos JT, Rodolfa KT, Niakan KK, Weisenthal LM, Mitsumoto H, Chung W, Croft GF, Saphier G, Leibel R, Goland R, Wichterle H, Henderson CE, Eggan K. Induced pluripotent stem cells generated from patients with ALS can be differentiated into motor neurons. *Science*, **321**, 1218–1221 (2008).
16) Hochedlinger K, Plath K. Epigenetic reprogramming and induced pluripotency. *Development*, **136**, 509–523 (2009).
17) Meissner A. Epigenetic modifications in pluripotent and differentiated cells. *Nat. Biotechnol.*, **28**, 1079–1088 (2010).
18) Tanaka T, Takahashi K, Yamane M, Tomida S, Nakamura S, Oshima K, Niwa A, Nishikomori R, Kambe N, Hara H, Mitsuyama M, Morone N, Heuser JE, Yamamoto T, Watanabe A, Sato-Otsubo A, Ogawa S, Asaka I, Heike T, Yamanaka S, Nakahata T, Saito MK. Induced pluripotent stem cells from CINCA syndrome patients as a model for dissecting somatic mosaicism and drug discovery. *Blood*, **120**, 1299–1308 (2012).
19) Goldenberg I, Moss AJ. Long QT syndrome. *J. Am. Coll. Cardiol.*, **51**, 2291–2300 (2008).
20) Marbán E. Cardiac channelopathies. *Nature*, **415**, 213–218 (2002).
21) Takahashi K, Yamanaka S. Induction of pluripotent stem cells from mouse embryonic and adult fibroblast cultures by defined factors. *Cell*, **126**, 663–676 (2006).
22) Soldner F, Hockemeyer D, Beard C, Gao Q, Bell GW, Cook EG, Hargus G, Blak A, Cooper O, Mitalipova M, Isacson O, Jaenisch R. Parkinson's disease patient-derived induced pluripotent stem cells free of viral reprogramming factors. *Cell*, **136**, 964–977 (2009).
23) Seki T, Yuasa S, Oda M, Egashira T, Yae K, Kusumoto D, Nakata H, Tohyama S, Hashimoto H, Kodaira M, Okada Y, Seimiya H, Fusaki N, Hasegawa M, Fukuda K. Generation of induced pluripotent stem cells from human terminally differentiated circulating T cells. *Cell Stem Cell*, **7**, 11–14 (2010).
24) Maherali N, Hochedlinger K. Guidelines and techniques for the generation of induced pluripotent stem cells. *Cell Stem Cell*, **3**, 595–605 (2008).
25) Gore A, Li Z, Fung H-L, Young JE, Agarwal S, Antosiewicz-Bourget J, Canto I, Giorgetti A, Israel MA, Kiskinis E, Lee JH, Loh YH, Manos PD, Montserrat N, Panopoulos AD, Ruiz S, Wilbert ML, Yu J, Kirkness EF, Izpisua Belmonte JC, Rossi DJ, Thomson JA, Eggan K, Daley GQ, Goldstein LS, Zhang K. Somatic coding mutations in human induced pluripotent stem cells. *Nature*, **471**, 63–67 (2011).
26) Laurent LC, Ulitsky I, Slavin I, Tran H, Schork A, Morey R, Lynch C, Harness JV, Lee S, Barrero MJ, Ku S, Martynova M, Semechkin R, Galat V, Gottesfeld J, Izpisua Belmonte JC, Murry C, Keirstead HS, Park HS, Schmidt U, Laslett AL, Muller FJ, Nievergelt CM, Shamir R, Loring JF. Dynamic changes in the copy number of pluripotency and cell proliferation genes in human ESCs and iPSCs during reprogramming and time in culture. *Cell Stem Cell*, **8**, 106–118 (2011).
27) Mekhoubad S, Bock C, de Boer AS, Kiskinis E, Meissner A, Eggan K. Erosion of dosage compensation impacts human iPSC disease modeling. *Cell Stem Cell*, **10**, 595–609 (2012).
28) Ohi Y, Qin H, Hong C, Blouin L, Polo JM, Guo T, Qi Z, Downey SL, Manos PD, Rossi DJ, Yu J, Hebrok M, Hochedlinger K, Costello JF, Song JS, Ramalho-Santos M. Incomplete DNA methylation underlies a transcriptional memory of somatic cells in human iPS cells. *Nat. Cell Biol.*, **13**, 541–549 (2011).
29) Soldner F, Laganière J, Cheng AW, Hockemeyer D, Gao Q, Alagappan R, Khurana V, Golbe LI, Myers RH, Lindquist S, Zhang

L, Guschin D, Fong LK, Vu BJ, Meng X, Urnov FD, Rebar EJ, Gregory PD, Zhang HS, Jaenisch R. Generation of isogenic pluripotent stem cells differing exclusively at two early onset Parkinson point mutations. *Cell*, **146**, 318–331 (2011).

30) Ananiev G, Williams EC, Li H, Chang Q. Isogenic pairs of wild type and mutant induced pluripotent stem cell (iPSC) lines from Rett syndrome patients as *in vitro* disease model. *PLoS ONE*, **6**, e25255 (2011).

31) Srivastava D. Making or breaking the heart: from lineage determination to morphogenesis. *Cell*, **126**, 1037–1048 (2006).

32) Hu B-Y, Weick JP, Yu J, Ma LX, Zhang XQ, Thomson JA, Zhang SC. Neural differentiation of human induced pluripotent stem cells follows developmental principles but with variable potency. *Proc. Natl. Acad. Sci. U.S.A.*, **107**, 4335–4340 (2010).

33) Kattman SJ, Witty AD, Gagliardi M, Dubois NC, Niapour M, Hotta A, Ellis J, Keller G. Stage-specific optimization of activin/nodal and BMP signaling promotes cardiac differentiation of mouse and human pluripotent stem cell lines. *Cell Stem Cell*, **8**, 228–240 (2011).

34) Polo JM, Liu S, Figueroa ME, Kulalert W, Eminli S, Tan KY, Apostolou E, Stadtfeld M, Li Y, Shioda T, Natesan S, Wagers AJ, Melnick A, Evans T, Hochedlinger K. Cell type of origin influences the molecular and functional properties of mouse induced pluripotent stem cells. *Nat. Biotechnol.*, **28**, 848–855 (2010).

35) Kim K, Doi A, Wen B, Ng K, Zhao R, Cahan P, Kim J, Aryee MJ, Ji H, Ehrlich LI, Yabuuchi A, Takeuchi A, Cunniff KC, Hongguang H, McKinney-Freeman S, Naveiras O, Yoon TJ, Irizarry RA, Jung N, Seita J, Hanna J, Murakami P, Jaenisch R, Weissleder R, Orkin SH, Weissman IL, Feinberg AP, Daley GQ. Epigenetic memory in induced pluripotent stem cells. *Nature*, **467**, 285–290 (2010).

36) Kim K, Zhao R, Doi A, Ng K, Unternaehrer J, Cahan P, Huo H, Loh YH, Aryee MJ, Lensch MW, Li H, Collins JJ, Feinberg AP, Daley GQ. Donor cell type can influence the epigenome and differentiation potential of human induced pluripotent stem cells. *Nat. Biotechnol.*, **29**, 1117–1119 (2011).

37) Hattori F, Chen H, Yamashita H, Tohyama S, Satoh YS, Yuasa S, Li W, Yamakawa H, Tanaka T, Onitsuka T, Shimoji K, Ohno Y, Egashira T, Kaneda R, Murata M, Hidaka K, Morisaki T, Sasaki E, Suzuki T, Sano M, Makino S, Oikawa S, Fukuda K. Nongenetic method for purifying stem cell-derived cardiomyocytes. *Nat. Methods*, **7**, 61–66 (2010).

38) Dubois NC, Craft AM, Sharma P, Elliott DA, Stanley EG, Elefanty AG, Gramolini A, Keller G. SIRPA is a specific cell-surface marker for isolating cardiomyocytes derived from human pluripotent stem cells. *Nat. Biotechnol.*, **29**, 1011–1018 (2011).

39) Nelson TJ, Martinez-Fernandez A, Terzic A. Induced pluripotent stem cells: developmental biology to regenerative medicine. *Nat. Rev. Cardiol.*, **7**, 700–710 (2010).

40) Blazeski A, Zhu R, Hunter DW, Weinberg SH, Zambidis ET, Tung L. Cardiomyocytes derived from human induced pluripotent stem cells as models for normal and diseased cardiac electrophysiology and contractility. *Prog. Biophys. Mol. Biol.*, **110**, 166–177 (2012).

41) Szabo E, Rampalli S, Risueño RM, Schnerch A, Mitchell R, Fiebig-Comyn A, Levadoux-Martin M, Bhatia M. Direct conversion of human fibroblasts to multilineage blood progenitors. *Nature*, **468**, 521–526 (2010).

42) Ambasudhan R, Talantova M, Coleman R, Yuan X, Zhu S, Lipton SA, Ding S. Direct reprogramming of adult human fibroblasts to functional neurons under defined conditions. *Cell Stem Cell*, **9**, 113–118 (2011).

43) Qiang L, Fujita R, Yamashita T, Angulo S, Rhinn H, Rhee D, Doege C, Chau L, Aubry L, Vanti WB, Moreno H, Abeliovich A. Directed conversion of Alzheimer's disease patient skin fibroblasts into functional neurons. *Cell*, **146**, 359–371 (2011).

44) Koch P, Tamboli IY, Mertens J, Wunderlich P, Ladewig J, Stüber K, Esselmann H, Wiltfang J, Brüstle O, Walter J. Presenilin-1 L166P mutant human pluripotent stem cell-derived neurons exhibit partial loss of γ-secretase activity in endogenous amyloid-β generation. *Am. J. Pathol.*, **180**, 2404–2416 (2012).

45) Nguyen HN, Byers B, Cord B, Shcheglovitov A, Byrne J, Gujar P, Kee K, Schüle B, Dolmetsch RE, Langston W, Palmer TD, Pera RR. LRRK2 mutant iPSC-derived DA neurons demonstrate increased susceptibility to oxidative stress. *Cell Stem Cell*, **8**, 267–280 (2011).

46) Itzhaki I, Maizels L, Huber I, Gepstein A, Arbel G, Caspi O, Miller L, Belhassen B, Nof E, Glikson M, Gepstein L. Modeling of catecholaminergic polymorphic ventricular tachycardia with patient-specific human-induced pluripotent stem cells. *J. Am. Coll. Cardiol.*, **60**, 990–1000 (2012).

47) Sun N, Yazawa M, Liu J, Han L, Sanchez-Freire V, Abilez OJ, Navarrete EG, Hu S, Wang L, Lee A, Pavlovic A, Lin S, Chen R, Hajjar RJ, Snyder MP, Dolmetsch RE, Butte MJ, Ashley EA, Longaker MT, Robbins RC, Wu JC. Patient-specific induced pluripotent stem cells as a model for familial dilated cardiomyopathy. *Sci. Transl. Med.*, **4**, ra47 (2012).

48) Rashid ST, Corbineau S, Hannan N, Marciniak SJ, Miranda E, Alexander G, Huang-Doran I, Griffin J, Ahrlund-Richter L, Skepper J, Semple R, Weber A, Lomas DA, Vallier L. Modeling inherited metabolic disorders of the liver using human induced pluripotent stem cells. *J. Clin. Invest.*, **120**, 3127–3136 (2010).

49) Kumano K, Arai S, Hosoi M, Taoka K, Takayama N, Otsu M, Nagae G, Ueda K, Nakazaki K, Kamikubo Y, Eto K, Aburatani H, Nakauchi H, Kurokawa M. Generation of induced pluripotent stem cells from primary chronic myelogenous leukemia patient samples. *Blood*, **119**, 6234–6242 (2012).

50) Fujikura J, Nakao K, Sone M, Noguchi M, Mori E, Naito M, Taura D, Harada-Shiba M, Kishimoto I, Watanabe A, Asaka I, Hosoda K, Nakao K. Induced pluripotent stem cells generated from diabetic patients with mitochondrial DNA A3243G mutation. *Diabetologia*, **55**, 1689–1698 (2012).

51) Shi Y, Kirwan P, Smith J, MacLean G, Orkin SH, Livesey FJ. A human stem cell model of early Alzheimer's disease pathology in Down syndrome. *Sci. Transl. Med.*, **4**, ra29 (2012).

52) Batista LFZ, Pech MF, Zhong FL, Nguyen HN, Xie KT, Zaug AJ, Crary SM, Choi J, Sebastiano V, Cherry A, Giri N, Wernig M, Alter BP, Cech TR, Savage SA, Reijo Pera RA, Artandi SE. Telomere shortening and loss of self-renewal in dyskeratosis congenita induced pluripotent stem cells. *Nature*, **474**, 399–402 (2011).

53) Agarwal S, Loh Y-H, McLoughlin EM, Huang J, Park IH, Miller JD, Huo H, Okuka M, Dos Reis RM, Loewer S, Ng HH, Keefe DL, Goldman FD, Klingelhutz AJ, Liu L, Daley GQ. Telomere elongation in induced pluripotent stem cells from dyskeratosis congenita patients. *Nature*, **464**, 292–296 (2010).

54) Jin Z-B, Okamoto S, Osakada F, Homma K, Assawachananont J, Hirami Y, Iwata T, Takahashi M. Modeling retinal degeneration using patient-specific induced pluripotent stem cells. *PLoS ONE*, **6**, e17084 (2011).

55) Mazzulli JR, Xu Y-H, Sun Y, Knight AL, McLean PJ, Caldwell GA, Sidransky E, Grabowski GA, Krainc D. Gaucher disease glucocerebrosidase and α-synuclein form a bidirectional pathogenic loop in synucleinopathies. *Cell*, **146**, 37–52 (2011).

56) Israel MA, Yuan SH, Bardy C, Reyna SM, Mu Y, Herrera C, Hefferan MP, Van Gorp S, Nazor KL, Boscolo FS, Carson CT, Laurent LC, Marsala M, Gage FH, Remes AM, Koo EH, Goldstein LS. Probing sporadic and familial Alzheimer's disease using induced pluripotent stem cells. *Nature*, **482**, 216–220 (2012).

57) Cohen JD, Babiarz JE, Abrams RM, Guo L, Kameoka S, Chiao E, Taunton J, Kolaja KL. Use of human stem cell derived cardiomyocytes to examine sunitinib mediated cardiotoxicity and electrophysiological alterations. *Toxicol. Appl. Pharmacol.*, **257**, 74–83 (2011).

58) Tanaka T, Tohyama S, Murata M, Nomura F, Kaneko T, Chen H, Hattori F, Egashira T, Seki T, Ohno Y, Koshimizu U, Yuasa

S, Ogawa S, Yamanaka S, Yasuda K, Fukuda K. *In vitro* pharmacologic testing using human induced pluripotent stem cell-derived cardiomyocytes. *Biochem. Biophys. Res. Commun.*, **385**, 497–502 (2009).

59) Zhang J, Wilson GF, Soerens AG, Koonce CH, Yu J, Palecek SP, Thomson JA, Kamp TJ. Functional cardiomyocytes derived from human induced pluripotent stem cells. *Circ. Res.*, **104**, e30–e41 (2009).

60) Germanguz I, Sedan O, Zeevi-Levin N, Shtrichman R, Barak E, Ziskind A, Eliyahu S, Meiry G, Amit M, Itskovitz-Eldor J, Binah O. Molecular characterization and functional properties of cardiomyocytes derived from human inducible pluripotent stem cells. *J. Cell. Mol. Med.*, **15**, 38–51 (2011).

61) Zeevi-Levin N, Itskovitz-Eldor J, Binah O. Cardiomyocytes derived from human pluripotent stem cells for drug screening. *Pharmacol. Ther.*, **134**, 180–188 (2012).

62) Moretti A, Bellin M, Welling A, Jung CB, Lam JT, Bott-Flügel L, Dorn T, Goedel A, Höhnke C, Hofmann F, Seyfarth M, Sinnecker D, Schömig A, Laugwitz KL. Patient-specific induced pluripotent stem-cell models for long-QT syndrome. *N. Engl. J. Med.*, **363**, 1397–1409 (2010).

63) Itzhaki I, Maizels L, Huber I, Zwi-Dantsis L, Caspi O, Winterstern A, Feldman O, Gepstein A, Arbel G, Hammerman H, Boulos M, Gepstein L. Modelling the long QT syndrome with induced pluripotent stem cells. *Nature*, **471**, 225–229 (2011).

64) Matsa E, Rajamohan D, Dick E, Young L, Mellor I, Staniforth A, Denning C. Drug evaluation in cardiomyocytes derived from human induced pluripotent stem cells carrying a long QT syndrome type 2 mutation. *Eur. Heart J.*, **32**, 952–962 (2011).

65) Yazawa M, Hsueh B, Jia X, Pasca AM, Bernstein JA, Hallmayer J, Dolmetsch RE. Using induced pluripotent stem cells to investigate cardiac phenotypes in Timothy syndrome. *Nature*, **471**, 230–234 (2011).

66) Davis RP, Casini S, van den Berg CW, Hoekstra M, Remme CA, Dambrot C, Salvatori D, Oostwaard DW, Wilde AA, Bezzina CR, Verkerk AO, Freund C, Mummery CL. Cardiomyocytes derived from pluripotent stem cells recapitulate electrophysiological characteristics of an overlap syndrome of cardiac sodium channel disease. *Circulation*, **125**, 3079–3091 (2012).

67) Lahti AL, Kujala VJ, Chapman H, Koivisto AP, Pekkanen-Mattila M, Kerkelä E, Hyttinen J, Kontula K, Swan H, Conklin BR, Yamanaka S, Silvennoinen O, Aalto-Setälä K. Model for long QT syndrome type 2 using human iPS cells demonstrates arrhythmogenic characteristics in cell culture. *Dis. Model Mech.*, **5**, 220–230 (2012).

68) Chouabe C, Neyroud N, Richard P, Denjoy I, Hainque B, Romey G, Drici MD, Guicheney P, Barhanin J. Novel mutations in KvLQT1 that affect Iks activation through interactions with Isk. *Cardiovasc. Res.*, **45**, 971–980 (2000).

69) Zipes DP, Camm AJ, Borggrefe M, Buxton AE, Chaitman B, Fromer M, Gregoratos G, Klein G, Moss AJ, Myerburg RJ, Priori SG, Quinones MA, Roden DM, Silka MJ, Tracy C, Smith SC Jr, Jacobs AK, Adams CD, Antman EM, Anderson JL, Hunt SA, Halperin JL, Nishimura R, Ornato JP, Page RL, Riegel B, Blanc JJ, Budaj A, Dean V, Deckers JW, Despres C, Dickstein K, Lekakis J, McGregor K, Metra M, Morais J, Osterspey A, Tamargo JL, Zamorano JLAmerican College of Cardiology/American Heart Association Task Force, European Society of Cardiology Committee for Practice Guidelines, European Heart Rhythm Association, Heart Rhythm Society. ACC/AHA/ESC 2006 guidelines for management of patients with ventricular arrhythmias and the prevention of sudden cardiac death. *Circulation*, **114**, e385–e484 (2006).

70) Vyas H, Hejlik J, Ackerman MJ. Epinephrine QT stress testing in the evaluation of congenital long-QT syndrome: diagnostic accuracy of the paradoxical QT response. *Circulation*, **113**, 1385–1392 (2006).

71) Shimizu W, Noda T, Takaki H, Nagaya N, Satomi K, Kurita T, Suyama K, Aihara N, Sunagawa K, Echigo S, Miyamoto Y, Yoshimasa Y, Nakamura K, Ohe T, Towbin JA, Priori SG, Kamakura S. Diagnostic value of epinephrine test for genotyping LQT1, LQT2, and LQT3 forms of congenital long QT syndrome. *Heart Rhythm*, **1**, 276–283 (2004).

72) Napolitano C, Priori SG, Schwartz PJ, Bloise R, Ronchetti E, Nastoli J, Bottelli G, Cerrone M, Leonardi S. Genetic testing in the long QT syndrome: development and validation of an efficient approach to genotyping in clinical practice. *JAMA*, **294**, 2975–2980 (2005).

73) Hescheler J, Halbach M, Egert U, Lu ZJ, Bohlen H, Fleischmann BK, Reppel M. Determination of electrical properties of ES cell-derived cardiomyocytes using MEAs. *J. Electrocardiol.*, **37** (Suppl.), 110–116 (2004).

74) Roden DM, Abraham RL. Refining repolarization reserve. *Heart Rhythm*, **8**, 1756–1757 (2011).

75) Roden DM. Clinical practice. Long-QT syndrome. *N. Engl. J. Med.*, **358**, 169–176 (2008).

76) Fitzgerald PT, Ackerman MJ. Drug-induced torsades de pointes: the evolving role of pharmacogenetics. *Heart Rhythm*, **2** (Suppl.), S30–S37 (2005).

77) Prescott C. The business of exploiting induced pluripotent stem cells. *Philos. Trans. R. Soc. Lond. B Biol. Sci.*, **366**, 2323–2328 (2011).

Heart Vessels
DOI 10.1007/s00380-012-0314-x

ORIGINAL ARTICLE

Incidence of periprocedural myocardial infarction and cardiac biomarker testing after percutaneous coronary intervention in Japan: results from a multicenter registry

Takahide Arai · Shinsuke Yuasa · Hiroaki Miyata · Akio Kawamura · Yuichiro Maekawa · Shiro Ishikawa · Shigetaka Noma · Soushin Inoue · Yuji Sato · Shun Kohsaka · Keiichi Fukuda

Received: 10 September 2012 / Accepted: 30 November 2012
© Springer Japan 2012

Abstract Periprocedural myocardial infarction (pMI) is an important complication associated with percutaneous coronary intervention (PCI). However, data on the frequency of biomarker testing and the incidence of pMI remain unclear. Using the multicenter Japan Cardiovascular Database, we identified 2182 patients who underwent PCI without preprocedural cardiac biomarker elevation (silent ischemia, stable angina, or unstable angina without biomarker elevation) from September 2008 to August 2011. Of these, 550 patients (25.2 %) underwent cardiac biomarker testing within 6–24 h after PCI. The incidence of pMI was 2.7 % among all identified patients and 7.5 % among those who underwent cardiac marker testing. Of note, cardiac biomarker testing was performed more frequently than no testing in patients with a higher risk profile such as unstable angina (32.7 vs 24.7 %, $P < 0.001$), higher symptom scaling (28.2 vs 22.5 %, $P = 0.008$), urgent or emergent procedures (19.3 vs 15.0 %, $P = 0.022$ or 4.2 vs 1.0 %, $P < 0.001$, respectively), and type C lesion (31.3 vs 25.2 %, $P = 0.006$). Presentation with silent ischemia (odds ratio = 1.51, 95 % confidence interval (CI) 1.16–1.97) and nonemergent PCIs (odds ratio = 3.45, 95 % CI 1.79–6.67) were associated with no postprocedural cardiac biomarker testing. The real-world multicenter PCI registry in Japan revealed an incidence of 2.7 % for pMI; however, cardiac biomarkers were assessed in only 25.2 % of patients after PCI. The results suggest an underuse of postprocedural biomarker testing and room for procedural quality improvement, particularly in cases of silent ischemia and nonemergent cases.

Keywords Percutaneous coronary intervention · Cardiac biomarker testing · Periprocedural myocardial infarction · Quality metrics

Introduction

The association between percutaneous coronary intervention (PCI) and subsequent myonecrosis, termed periprocedural myocardial infarction (pMI), has long been recognized, with pMI occurring in 5 –30 % of patients after PCI [1–4]. In most cases, however, the pMI is clinically silent and could thus be underestimated if cardiac biomarkers are not measured routinely after PCI. Published guidelines cite the measurement of cardiac biomarkers in patients with signs or symptoms of myocardial infarction during or after PCI as a class I recommendation and the routine measurement of cardiac biomarkers in those who

T. Arai (✉) · S. Yuasa · A. Kawamura · Y. Maekawa · S. Kohsaka · K. Fukuda
Department of Cardiology, Keio University School of Medicine, 35 Shinanomachi, Shinjuku-ku, Tokyo 160-8582, Japan
e-mail: tarai@cpnet.med.keio.ac.jp

H. Miyata
Department of Healthcare Quality Assessment, Graduate School of Medicine, University of Tokyo, Tokyo, Japan

S. Ishikawa
Department of Cardiology, Saitama City Hospital, Saitama, Japan

S. Noma
Department of Cardiology, Saiseikai Utsunomiya Hospital, Utsunomiya, Japan

S. Inoue
Department of Cardiology, Hino City Hospital, Tokyo, Japan

Y. Sato
Center for Clinical Research, Keio University School of Medicine, Tokyo, Japan

Published online: 29 December 2012

have undergone complicated procedures as a class IIa recommendation [5]. In the United States, the reported overall frequency of cardiac biomarker testing after PCI is 24.7 %, with large institutional and regional variations [6]. However, the incidence of pMI and frequency of cardiac biomarker testing after PCI in Japan, where 200,000 procedures are performed each year, is unknown. In the present study, we investigated the important parameters used to identify the clinical variables associated with nonmeasurement of postprocedural biomarkers.

Patients and methods

Study design

The Japan Cardiovascular Database (JCD) is a large, ongoing prospective multicenter cohort study designed to collect clinical background and outcome data on PCI patients. Data were collected for approximately 5700 variables, with participating hospitals instructed to record data from consecutive hospital visits for PCI and to enter the relevant information into an internet-based database system. The system then checks the input data to ensure it is complete and internally consistent. PCI with any commercially available coronary device may be included. The decision to perform PCI was made according to the investigators' clinical assessment of the patient. The study did not mandate specific interventional or surgical techniques, such as vascular access, use of specific stents, or closure devices. The majority of clinical variables in the JCD were defined according to the National Cardiovascular Data Registry, sponsored by the American College of Cardiology.

Information disclosure

Before the launch of the JCD, information on the objectives of the present study, its social significance, and an abstract were provided for clinical trial registration with the University Hospital Medical Information Network, which is recognized by the International Committee of Medical Journal Editors as an "acceptable registry" according to a statement issued in September 2004 (UMIN R000005598). Written informed consent was obtained from all patients. The study protocol was approved by the Ethics Committee of Keio University.

Participants

Patients were enrolled by the event, and all consecutive PCI procedures during the study period, including failure cases, were registered. Patients under 18 years of age were excluded. A subgroup of patients who underwent intracoronary infusion of acetylcholine to induce coronary vasospasm was also registered, because vasospastic angina accounts for a significant portion of patients with coronary artery disease and acute coronary syndrome in Japan.

Procedures and data collection

The JCD began enrolling patients in September 2008. Only patients who underwent PCI were included in the present analysis; those who underwent an acetylcholine challenge test were excluded. We analyzed the data from 3894 patients undergoing PCI at 14 Japanese hospitals participating in the JCD Kumamoto Intervention Conference Study from September 2008 to August 2011. Of those 3894 patients, we analyzed 2182, excluding cases of acute myocardial infarction. These patients were divided into those with and without cardiac biomarker testing. We investigated the frequency of cardiac biomarker measurement and compared the predictors or outcome among patients with and without postprocedure cardiac biomarker testing. In-hospital complications were documented for each patient by the treating cardiologists. The clinical coordinator reported any lack of postprocedural information in the report, as mandated by the site data manager.

End points

The end points were defined as in-hospital mortality, heart failure, cardiogenic shock, and complications. Complications were defined as all possible complications, i.e., severe dissection or coronary perforation, myocardial infarction after PCI, cardiogenic shock or heart failure, cerebral bleeding or stroke, and bleeding complications. Myocardial infarction was defined as the new occurrence of a biomarker-positive myocardial infarction after PCI. At least one determination of biomarkers obtained no sooner than 6 h after PCI, and preferably within 6–24 h post-PCI, was used. In addition, Q waves with absent, incomplete, or inconclusive biomarkers were considered evidence of myocardial infarction. Bleeding complications in this registry were further defined as requiring transfusion and/or prolonging hospital stay and/or causing a decrease in hemoglobin levels below 3.0 g/dl. Furthermore, bleeding complications were divided into puncture-site bleeding, retroperitoneal bleeding, gastrointestinal bleeding, genitourinary bleeding, or other bleeding.

Statistical analysis

All statistical analyses were performed using SPSS version 15.0 (SPSS, Chicago, IL, USA). Continuous variables are expressed as mean $\pm$ standard deviation (SD) or the

corresponding interquartile range. Dichotomous variables are expressed as counts and percentages. For group comparison of continuous variables, a Student *t* test was used. A Chi-square test was also used to compare two proportions. Multivariable logistic regression was used to determine the factors independently associated with noncardiac biomarker testing in patients who underwent PCI. A *P* value of less than 0.05 was considered statistically significant.

Results

Patients' characteristics

Baseline clinical characteristics of the study group are shown in Table 1. Among the 2182 patients, 550 (25.2 %) had cardiac biomarker testing after PCI. Mean patient age in this group was 68.66 years; 105 patients were female (19.1 %); and the indications included silent ischemia in 145 patients (26.4 %), unstable angina in 180 patients (32.7 %), urgent PCI in 106 patients (19.3 %), and emergent PCI in 23 patients (4.2 %). Creatine kinase–muscle/brain (CK-MB) was measured in 543 patients (98.7 %) and troponin T was measured in 34 patients (6.2 %).

The rate of cardiac biomarker testing was higher than the rate of no testing among patients with unstable angina (32.7 vs 24.7 %), with high Canadian Cardiovascular Society presentation (28.2 vs 22.5 %), and with urgent and emergent procedures (19.3 vs 15.0 % and 4.2 vs 1.0 %, respectively), compared with those patients without either of these specific conditions. By contrast, the incidence of cardiac biomarker testing after PCI was significantly lower than that of no testing among patients with silent ischemia (26.4 vs 32.5 %).

Angiographic and procedural characteristics

Angiographic and procedural characteristics are detailed in Table 2. The incidence of cardiac biomarker testing was significantly higher than that of no testing among patients with type C lesions (31.3 vs 25.2 %), although other complex lesions, such as chronic total occlusion and left main trunk lesions, were not significantly associated with cardiac biomarker testing. As a procedural complication, perforation was associated with cardiac biomarker testing (2.2 vs 0.7 %).

Multivariate analysis

Multivariate analysis identified a high-risk feature, such as symptoms of heart failure, as an independent variable indicating cardiac biomarker testing (Table 3). By contrast, a low-risk feature such as nonemergent PCI was an independent variable indicating no cardiac biomarker testing.

Table 1 Baseline patient characteristics stratified by presentation of postprocedural biomarker testing

Characteristic	Marker testing (−) (*n* = 1632)	Marker testing (+) (*n* = 550)	*P* value
Patient background			
Age (years)	68.0 ± 9.9	68.7 ± 9.9	0.189
Gender (female)	329 (20.2 %)	105 (19.1 %)	0.621
BSA	1.68 ± 0.18	1.67 ± 0.19	0.615
BMI	24.9 ± 20.5	25.2 ± 21.8	0.769
Risk factors			
Diabetes	738 (45.2 %)	232 (42.2 %)	0.234
Dyslipidemia	1137 (69.7 %)	397 (72.2 %)	0.281
Hypertension	1255 (76.9 %)	423 (76.9 %)	1.000
Smoking	470 (28.8 %)	165 (30.0 %)	0.588
CKD	85 (5.2 %)	31 (5.6 %)	0.742
Hemodialysis	68 (4.2 %)	23 (4.2 %)	1.000
Malignancy	66 (4.0 %)	14 (2.5 %)	0.116
CVD	140 (8.6 %)	51 (9.3 %)	0.602
PVD	134 (8.2 %)	52 (9.5 %)	0.378
COPD	44 (2.7 %)	19 (3.5 %)	0.377
Previous myocardial infarction	509 (31.2 %)	173 (31.5 %)	0.915
Previous heart failure	155 (9.5 %)	48 (8.7 %)	0.671
Prior PCI	788 (48.3 %)	259 (47.1 %)	0.657
Prior CABG	117 (7.2 %)	30 (5.5 %)	0.201
Clinical presentation			
Silent ischemia	531 (32.5 %)	145 (26.4 %)	0.007
Stable angina	698 (42.8 %)	225 (40.9 %)	0.454
Unstable angina	403 (24.7 %)	180 (32.7 %)	<0.001
Symptoms of heart failure	139 (8.5 %)	62 (11.3 %)	0.060
>CCS 3	367 (22.5 %)	155 (28.2 %)	0.008
>NYHA III	59 (3.6 %)	30 (5.5 %)	0.062
Preprocedural medical angina treatment	431 (26.4 %)	135 (24.5 %)	0.399
Urgent PCI	245 (15.0 %)	106 (19.3 %)	0.022
Emergent PCI	16 (1.0 %)	23 (4.2 %)	<0.001
Noninvasive imaging test			
Exercise test	852 (52.2 %)	278 (50.5 %)	0.521
Coronary CT	387 (23.7 %)	139 (25.3 %)	0.454

BSA body surface area, *BMI* body mass index, *CKD* chronic kidney disease, *CVD* cerebrovascular disease, *PVD* peripheral vascular disease, *COPD* chronic obstructive pulmonary disease, *PCI* percutaneous coronary intervention, *CABG* coronary artery bypass graft, *CCS* Canadian Cardiovascular Society, *NYHA* New York Heart Association

In-hospital outcome

The in-hospital outcomes are detailed in Table 4. Overall in-hospital mortality was 0.5 %, cardiogenic shock was

Table 2 Angiographic and procedural characteristics

	Marker testing (−) (n = 1632)	Marker testing (+) (n = 550)	P value
Lesion characteristics			
Two-vessel disease	760 (46.6 %)	271 (49.3 %)	0.278
Three-vessel disease	406 (24.9 %)	141 (25.6 %)	0.733
Left main trunk	148 (9.1 %)	66 (12.0 %)	0.056
Bifurcation lesion	357 (21.9 %)	26 (14.3 %)	0.053
Type C lesion	411 (25.2 %)	172 (31.3 %)	0.006
Chronic total occlusion	130 (8.0 %)	37 (6.7 %)	0.404
Device used			
Plain old balloon angioplasty	199 (12.2 %)	55 (10.0 %)	0.191
Bare metal stent	263 (16.1 %)	91 (16.5 %)	0.841
Drug-eluting stent	621 (38.1 %)	202 (36.7 %)	0.611
Intra-aortic balloon pumping	13 (0.8 %)	9 (1.6 %)	0.134
Intravascular ultrasound	630 (38.6 %)	216 (39.3 %)	0.800
Postprocedural TIMI flow under grade 3	41 (2.5 %)	19 (3.5 %)	0.290
Procedural complication			
Perforation	11 (0.7 %)	12 (2.2 %)	0.006
Dissection	20 (1.2 %)	10 (1.8 %)	0.295

Table 3 Factors associated with noncardiac biomarker testing after PCI

Variable	Odds ratio	95 % CI	P value
Nonemergent PCI	3.45	1.79–6.67	<0.001
Silent ischemia	1.51	1.16–1.97	0.002
Heart failure	0.71	0.51–0.98	0.037
Stable angina	1.27	1.00–1.62	0.05
Left main trunk	0.73	0.53–1.00	0.05

Table 4 In-hospital outcomes

	All (n = 2182)	Marker testing (−) (n = 1632)	Marker testing (+) (n = 550)	P value
Death	11 (0.5 %)	9 (0.6 %)	2 (0.4 %)	0.741
Cardiogenic shock	15 (0.7 %)	9 (0.6 %)	6 (1.1 %)	0.229
Myocardial infarction (pMI)	59 (2.7 %)	18 (1.1 %)	41 (7.5 %)	<0.001
Contrast nephropathy	131 (6.0 %)	84 (5.1 %)	47 (8.5 %)	0.005
Bleeding	47 (2.2 %)	21 (2.1 %)	26 (6.3 %)	<0.001
Transfusion	34 (1.6 %)	18 (1.1 %)	16 (2.9 %)	0.005

0.7 %, and pMI was 2.7 %. In-hospital mortality rate and cardiogenic shock did not differ between the tested and untested groups (0.4 vs 0.6 %, $P = 0.741$ and 1.1 vs 0.6 %, $P = 0.229$, respectively), although the incidence was very low for both outcomes. The frequency of cardiac biomarker testing was significantly higher among patients with pMI (7.5 vs 1.1 %). The incidence of cardiac biomarker testing was significantly higher than that of no testing among patients with contrast nephropathy (8.5 vs 5.1 %), bleeding (2.1 vs 6.3 %), and transfusion (2.9 vs 1.1 %).

Discussion

The major findings of the present study based on the JCD database were as follows: (1) the incidence of pMI among patients undergoing PCI was 2.7 %, but cardiac biomarkers were assessed in only 25.2 % of patients after PCI; (2) cardiac biomarker testing was performed more frequently in patients with a higher risk profile; and (3) similar rates of in-hospital complications between tested and untested patients implies the underuse of postprocedural biomarker testing and the probable need for procedural quality improvement, particularly in cases of silent ischemia and non-emergent cases.

Although pMI occurs in 5 –30 % of patients after PCI [2–4], the clinical significance and clinical outcome of pMI remain controversial [7–9]. The general conclusion based on previous retrospective analyses is that significant myocardial damage is associated with a poor outcome [10, 11], and a recent report revealed that an increase in CK-MB to greater than 10 times the upper limit of normal is associated with a marked and progressive increase in the 1-year mortality rate [12]. Current guidelines recommend that patients with a periprocedural CK-MB elevation greater than 3 times the upper limit of normal should be treated for standard myocardial infarction [13–16]. Thus, pMI is often treated similarly to spontaneous myocardial infarction in clinical trials [17], although the current universal definition of myocardial infarction attempts to create a specific category (type 4a) for pMI to distinguish it from spontaneous myocardial infarction (type 1 and 2) [13]. In the present study, the incidence of pMI was 2.7 %, which is significantly lower than that in previous reports. Cardiac biomarker testing was performed in only 25.2 % of patients after PCI in the JCD registry cases. Thus, because most pMIs are clinically silent, the incidence of pMI might be underestimated using this approach.

Here we sought to identify factors associated with noncardiac biomarker testing after PCI. Nonemergent PCI was an independent variable of noncardiac biomarker testing, and in general such patients maintained a stable clinical condition without symptoms during or after PCI,

even in the presence of a small myocardial infarction. Thus, the indication for cardiac biomarker testing mainly depends on the disease state and PCI, rather than the periprocedural factors mentioned in the guidelines.

Predictors of pMI are reported to be emergent situations, complex lesions (such as the presence of thrombus and a type C lesion), complex procedures (such as the use of rotational atherectomy), and associated complications [18–21]. In the present study, the incidence of an emergent PCI, a type C lesion and complications such as perforation were higher in the cardiac marker-tested group, leading to a higher incidence of pMI in the group tested for cardiac markers.

In this study, although the occurrence of pMI was lower in the noncardiac biomarker testing group than in the cardiac biomarker testing group, the occurrence of in-hospital mortality and cardiogenic shock did not differ between groups. pMI is a suggested quality metric for PCI care [22]; however, because most pMIs are clinically silent, routine cardiac biomarker testing should be performed to detect pMI more precisely, and the occurrence of pMI might actually be underestimated in our nonbiomarker group. In addition, measurement of cardiac biomarkers leads to the detection of other complications and intensive care after PCI. Indeed, our biomarker assessment group showed a high rate of complications, such as contrast nephropathy and bleeding, as well as a higher frequency of transfusion. Biomarker assessment leads to a higher probability of intensive care in comparison with patients in the noncardiac biomarker testing group. Renal insufficiency and anemia are reported to be associated with major cardiac and cerebrovascular events after PCI [23]. Therefore, intensive care is needed to improve outcomes after PCI. Together, these findings indicate that pMI is a suitable quality metric for the care of patients after PCI, and thus more precise detection of pMI could lead to improved outcomes for patients undergoing PCI.

Study limitations

This was a retrospective observational study. In addition, the registry data did not include the degree of the increase in CK-MB and troponin T, or long-term outcomes. Further studies with quantitative analysis and long-term follow-up are needed to assess the effects of pMI.

Conclusions

These findings from the multicenter PCI registry in Japan suggested the underuse of postprocedural biomarker testing. Based on these findings, stronger recommendations for such testing should be made, particularly in cases of silent ischemia and nonemergent cases.

Acknowledgments This study was supported by the Grant-in-Aid for Scientific Research from SENSHIN Medical Research Foundation and Pfizer Health Research Foundation (to S.K.).

Conflict of interest None.

References

1. Califf RM, Abdelmeguid AE, Kuntz RE, Popma JJ, Davidson CJ, Cohen EA, Kleiman NS, Mahaffey KW, Topol EJ, Pepine CJ, Lipicky RJ, Granger CB, Harrington RA, Tardiff BE, Crenshaw BS, Bauman RP, Zuckerman BD, Chaitman BR, Bittl JA, Ohman EM (1998) Myonecrosis after revascularization procedures. J Am Coll Cardiol 31(2):241–251
2. Herrmann J (2005) Peri-procedural myocardial injury: 2005 update. Eur Heart J 26(23):2493–2519
3. Porto I, Selvanayagam JB, Van Gaal WJ, Prati F, Cheng A, Channon K, Neubauer S, Banning AP (2006) Plaque volume and occurrence and location of periprocedural myocardial necrosis after percutaneous coronary intervention: insights from delayed-enhancement magnetic resonance imaging, thrombolysis in myocardial infarction myocardial perfusion grade analysis, and intravascular ultrasound. Circulation 114(7):662–669
4. Prasad A, Herrmann J (2011) Myocardial infarction due to percutaneous coronary intervention. N Engl J Med 364(5):453–464
5. Smith SC Jr, Feldman TE, Hirshfeld JW Jr, Jacobs AK, Kern MJ, King SB 3rd, Morrison DA, O'Neil WW, Schaff HV, Whitlow PL, Williams DO, Antman EM, Adams CD, Anderson JL, Faxon DP, Fuster V, Halperin JL, Hiratzka LF, Hunt SA, Nishimura R, Ornato JP, Page RL, Riegel B (2006) ACC/AHA/SCAI 2005 guideline update for percutaneous coronary intervention: a report of the American College of Cardiology/American Heart Association Task Force on Practice Guidelines (ACC/AHA/SCAI Writing Committee to Update 2001 Guidelines for Percutaneous Coronary Intervention). Circulation 113(7):e166–e286
6. Wang TY, Peterson ED, Dai D, Anderson HV, Rao SV, Brindis RG, Roe MT (2008) Patterns of cardiac marker surveillance after elective percutaneous coronary intervention and implications for the use of periprocedural myocardial infarction as a quality metric: a report from the National Cardiovascular Data Registry (NCDR). J Am Coll Cardiol 51(21):2068–2074
7. Bhatt DL, Topol EJ (2005) Does creatinine kinase-MB elevation after percutaneous coronary intervention predict outcomes in 2005? Periprocedural cardiac enzyme elevation predicts adverse outcomes. Circulation 112(6):906–915 (discussion 23)
8. Cutlip DE, Kuntz RE (2005) Does creatinine kinase-MB elevation after percutaneous coronary intervention predict outcomes in 2005? Cardiac enzyme elevation after successful percutaneous coronary intervention is not an independent predictor of adverse outcomes. Circulation 112(6):916–922 (discussion 22)
9. Prasad A, Rihal CS, Lennon RJ, Singh M, Jaffe AS, Holmes DR Jr (2008) Significance of periprocedural myonecrosis on outcomes after percutaneous coronary intervention: an analysis of preintervention and postintervention troponin T levels in 5487 patients. Circ Cardiovasc Interv 1(1):10–19
10. Stone GW, Mehran R, Dangas G, Lansky AJ, Kornowski R, Leon MB (2001) Differential impact on survival of electrocardiographic Q-wave versus enzymatic myocardial infarction after percutaneous intervention: a device-specific analysis of 7147 patients. Circulation 104(6):642–647

11. Ellis SG, Chew D, Chan A, Whitlow PL, Schneider JP, Topol EJ (2002) Death following creatine kinase-MB elevation after coronary intervention: identification of an early risk period: importance of creatine kinase-MB level, completeness of revascularization, ventricular function, and probable benefit of statin therapy. Circulation 106(10):1205–1210
12. Novack V, Pencina M, Cohen DJ, Kleiman NS, Yen CH, Saucedo JF, Berger PB, Cutlip DE (2012) Troponin criteria for myocardial infarction after percutaneous coronary intervention. Arch Intern Med 172(6):502–508
13. Thygesen K, Alpert JS, White HD, Jaffe AS, Apple FS, Galvani M, Katus HA, Newby LK, Ravkilde J, Chaitman B, Clemmensen PM, Dellborg M, Hod H, Porela P, Underwood R, Bax JJ, Beller GA, Bonow R, Van der Wall EE, Bassand JP, Wijns W, Ferguson TB, Steg PG, Uretsky BF, Williams DO, Armstrong PW, Antman EM, Fox KA, Hamm CW, Ohman EM, Simoons ML, Poole-Wilson PA, Gurfinkel EP, Lopez-Sendon JL, Pais P, Mendis S, Zhu JR, Wallentin LC, Fernandez-Aviles F, Fox KM, Parkhomenko AN, Priori SG, Tendera M, Voipio-Pulkki LM, Vahanian A, Camm AJ, De Caterina R, Dean V, Dickstein K, Filippatos G, Funck-Brentano C, Hellemans I, Kristensen SD, McGregor K, Sechtem U, Silber S, Widimsky P, Zamorano JL, Morais J, Brener S, Harrington R, Morrow D, Lim M, Martinez-Rios MA, Steinhubl S, Levine GN, Gibler WB, Goff D, Tubaro M, Dudek D, Al-Attar N (2007) Universal definition of myocardial infarction. Circulation 116(22):2634–2653
14. Smith SC Jr, Feldman TE, Hirshfeld JW Jr, Jacobs AK, Kern MJ, King SB 3rd, Morrison DA, O'Neill WW, Schaff HV, Whitlow PL, Williams DO, Antman EM, Adams CD, Anderson JL, Faxon DP, Fuster V, Halperin JL, Hiratzka LF, Hunt SA, Nishimura R, Ornato JP, Page RL, Riegel B (2006) ACC/AHA/SCAI 2005 guideline update for percutaneous coronary intervention—summary article: a report of the American College of Cardiology/American Heart Association Task Force on Practice Guidelines (ACC/AHA/SCAI Writing Committee to Update the 2001 Guidelines for Percutaneous Coronary Intervention). J Am Coll Cardiol 47(1):216–235
15. King SB 3rd, Smith SC Jr, Hirshfeld JW Jr, Jacobs AK, Morrison DA, Williams DO, Feldman TE, Kern MJ, O'Neill WW, Schaff HV, Whitlow PL, Adams CD, Anderson JL, Buller CE, Creager MA, Ettinger SM, Halperin JL, Hunt SA, Krumholz HM, Kushner FG, Lytle BW, Nishimura R, Page RL, Riegel B, Tarkington LG, Yancy CW (2008) 2007 focused update of the ACC/AHA/SCAI 2005 guideline update for percutaneous coronary intervention: a report of the American College of Cardiology/American Heart Association Task Force on Practice guidelines. J Am Coll Cardiol 51(2):172–209
16. Song YB, Lee SY, Hahn JY, Choi SH, Choi JH, Lee SH, Hong KP, Park JE, Gwon HC (2012) Complete versus incomplete revascularization for treatment of multivessel coronary artery disease in the drug-eluting stent era. Heart Vessels 27(5):433–442
17. Bhatt DL, Lincoff AM, Gibson CM, Stone GW, McNulty S, Montalescot G, Kleiman NS, Goodman SG, White HD, Mahaffey KW, Pollack CV Jr, Manoukian SV, Widimsky P, Chew DP, Cura F, Manukov I, Tousek F, Jafar MZ, Arneja J, Skerjanec S, Harrington RA (2009) Intravenous platelet blockade with cangrelor during PCI. N Engl J Med 361(24):2330–2341
18. Mandadi VR, DeVoe MC, Ambrose JA, Prakash AM, Varshneya N, Gould RB, Nguyen TH, Geagea JP, Radojevic JA, Sehhat K, Barua RS (2004) Predictors of troponin elevation after percutaneous coronary intervention. Am J Cardiol 93(6):747–750
19. Blankenship JC, Haldis T, Feit F, Hu T, Kleiman NS, Topol EJ, Lincoff AM (2006) Angiographic adverse events, creatine kinase-MB elevation, and ischemic end points complicating percutaneous coronary intervention (a REPLACE-2 substudy). Am J Cardiol 97(11):1591–1596
20. Cai Q, Skelding KA, Armstrong AT Jr, Desai D, Wood GC, Blankenship JC (2007) Predictors of periprocedural creatine kinase-myocardial band elevation complicating elective percutaneous coronary intervention. Am J Cardiol 99(5):616–620
21. van Gaal WJ, Ponnuthurai FA, Selvanayagam J, Testa L, Porto I, Neubauer S, Banning AP (2009) The Syntax score predicts periprocedural myocardial necrosis during percutaneous coronary intervention. Int J Cardiol 135(1):60–65
22. Moscucci M, Rogers EK, Montoye C, Smith DE, Share D, O'Donnell M, Maxwell-Eward A, Meengs WL, De Franco AC, Patel K, McNamara R, McGinnity JG, Jani SM, Khanal S, Eagle KA (2006) Association of a continuous quality improvement initiative with practice and outcome variations of contemporary percutaneous coronary interventions. Circulation 113(6):814–822
23. Matsue Y, Matsumura A, Abe M, Ono M, Seya M, Nakamura T, Iwatsuka R, Mizukami A, Setoguchi M, Nagahori W, Ohno M, Suzuki M, Hashimoto Y (2012) Prognostic implications of chronic kidney disease and anemia after percutaneous coronary intervention in acute myocardial infarction patients. Heart Vessels. doi:10.1007/s00380-011-0209-2

Cell PRESS

Distinct Metabolic Flow Enables Large-Scale Purification of Mouse and Human Pluripotent Stem Cell-Derived Cardiomyocytes

Shugo Tohyama,[1,3] Fumiyuki Hattori,[1,4,*] Motoaki Sano,[1] Takako Hishiki,[2] Yoshiko Nagahata,[2,5] Tomomi Matsuura,[2,5] Hisayuki Hashimoto,[1] Tomoyuki Suzuki,[6] Hiromi Yamashita,[1,4] Yusuke Satoh,[1] Toru Egashira,[1] Tomohisa Seki,[1] Naoto Muraoka,[1] Hiroyuki Yamakawa,[1] Yasuyuki Ohgino,[1] Tomofumi Tanaka,[4] Masatoshi Yoichi,[4] Shinsuke Yuasa,[1] Mitsushige Murata,[1] Makoto Suematsu,[2,5] and Keiichi Fukuda[1,*]
[1]Department of Cardiology
[2]Department of Biochemistry
Keio University School of Medicine, Tokyo 160-8582, Japan
[3]Japan Society for the Promotion of Science, Tokyo 102-8472, Japan
[4]Asubio Pharma, Kobe 650-0047, Japan
[5]Japan Science and Technology Agency (JST), Exploratory Research for Advanced Technology (ERATO) Suematsu Gas Biology Project, Tokyo 160-8582, Japan
[6]Department of Cardiovascular Research, Research Institute of Environmental Medicine, Nagoya University, Nagoya 464-8601, Japan
*Correspondence: hattori.fumiyuki.ef@asubio.co.jp (F.H.), kfukuda@a2.keio.jp (K.F.)
http://dx.doi.org/10.1016/j.stem.2012.09.013

SUMMARY

Heart disease remains a major cause of death despite advances in medical technology. Heart-regenerative therapy that uses pluripotent stem cells (PSCs) is a potentially promising strategy for patients with heart disease, but the inability to generate highly purified cardiomyocytes in sufficient quantities has been a barrier to realizing this potential. Here, we report a nongenetic method for mass-producing cardiomyocytes from mouse and human PSC derivatives that is based on the marked biochemical differences in glucose and lactate metabolism between cardiomyocytes and noncardiomyocytes, including undifferentiated cells. We cultured PSC derivatives with glucose-depleted culture medium containing abundant lactate and found that only cardiomyocytes survived. Using this approach, we obtained cardiomyocytes of up to 99% purity that did not form tumors after transplantation. We believe that our technological method broadens the range of potential applications for purified PSC-derived cardiomyocytes and could facilitate progress toward PSC-based cardiac regenerative therapy.

INTRODUCTION

Heart disease is a common and deadly disease, and heart-regenerative therapy is a promising therapeutic strategy for some patients (Passier et al., 2008). Pluripotent stem cells (PSCs) including embryonic stem cells (ESCs) and induced pluripotent stem cells (iPSCs) are potential sources for production of therapeutic cardiomyocytes (Burridge et al., 2012; Takahashi et al., 2007; Thomson et al., 1998). A typical human left ventricle contains roughly 6×10^9 cardiomyocytes; thus, nearly 1×10^9 de novo cardiomyocytes would be required per patient for this type of repair (Hattori and Fukuda, 2012). However, PSC-based approaches carry a high risk of tumor formation due to contamination of residual PSCs in the therapeutic cell preparations. Therefore, obtaining highly purified cardiomyocytes will be key for achieving therapeutic success in applying these cells.

Procedures involving density-gradient centrifugation (Laflamme et al., 2007; Xu et al., 2006), genetic modification (Fijnvandraat et al., 2003; Gassanov et al., 2004; Hidaka et al., 2003; Klug et al., 1996), and nongenetic methods that use a mitochondrial dye (Hattori et al., 2010) or antibodies to specific cell-surface markers (Dubois et al., 2011; Uosaki et al., 2011) have been established for cardiomyocyte enrichment. However, none of these methods are ideal for the therapeutic application of PSC-derived cardiomyocytes because of drawbacks including insufficient purity, genotoxicity, and the use of fluorescence-activated cell sorting (FACS) and/or antibodies.

Glucose is the main source of energy and anabolic precursors in various mammalian cells. It is converted by glycolysis into pyruvate and/or lactate via glucose-6-phosphate (G6P; a source of nucleotides) and 3-phosphoglycerate (a source of some amino acids) for generation of two ATP molecules without the need for oxygen. Pyruvate is further utilized in the mitochondrial tricarboxylic acid (TCA) cycle for production of 36 ATP molecules via oxidative phosphorylation (OXPHOS). Cardiomyocytes efficiently produce energy from several substrates including glucose, fatty acids, and lactate via OXPHOS. Interestingly, there are marked changes between energy substrate utilization by cardiomyocytes before and after birth. The fetal heart has a higher capacity for lactate uptake than the adult heart (Fisher et al., 1981) and uses lactate as a major energy source (Neely and Morgan, 1974; Werner and Sicard, 1987) by exploiting the lactate-rich environment created by the placenta (Burd et al., 1975).

In this study, we took advantage of the unique metabolic properties of cardiomyocytes to develop an efficient and

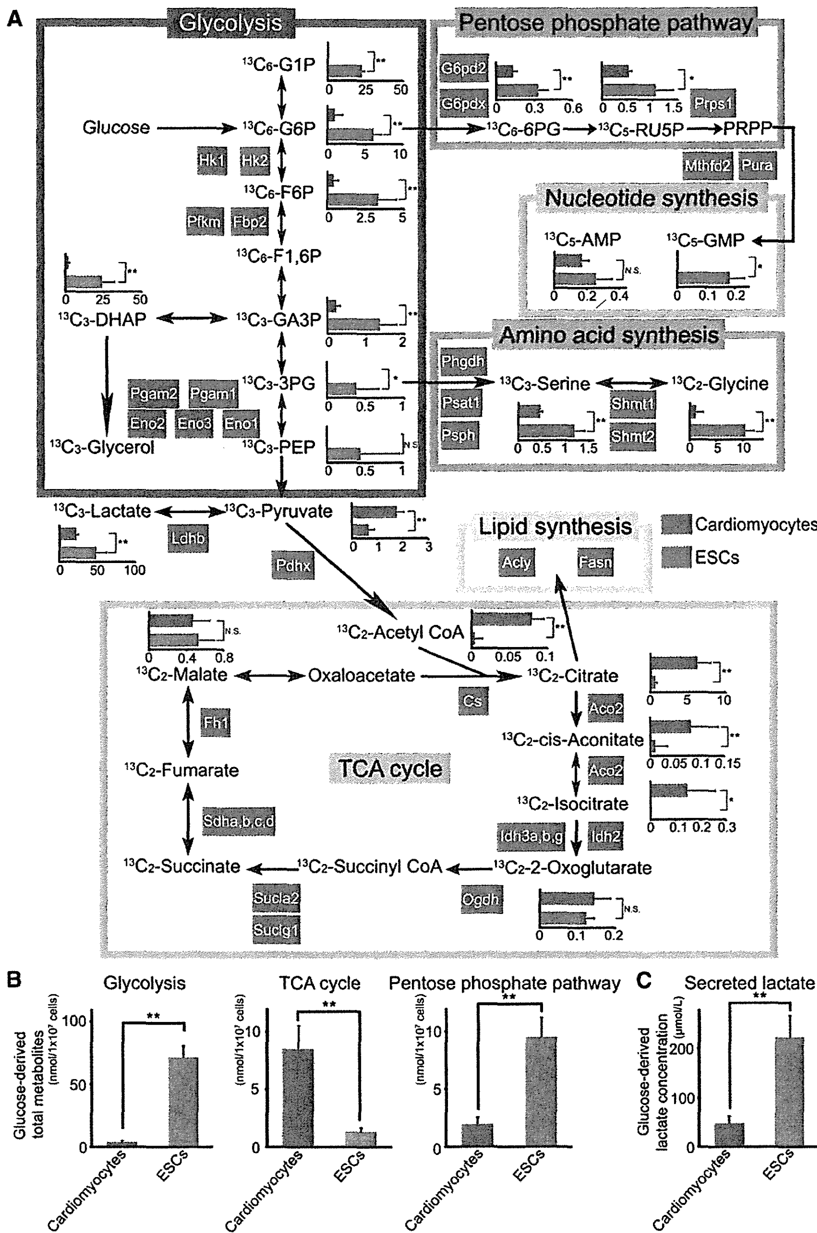

Figure 1. Distinct Metabolic Differences Between Cardiomyocytes and ESCs in *Transcriptome and Fluxome Analyses*

(A) Metabolic pathway map summarizing the results from gene array and [^{13}C]-labeled glucose fluxome analyses. Gene names shown in red or blue boxes indicate the mRNA expression levels increased more than 2-fold in cardiomyocytes or ESCs, respectively. The bar graphs represent the detected levels of [^{13}C]-labeled metabolites in cardiomyocytes (red bar) and ESCs (blue bar) (n = 4). All units are nmol per 1.0×10^7 cells. All data were obtained from independent experiments.

(B) Total [^{13}C]-labeled metabolites of cardiomyocytes (red bar) and ESCs (blue bar) in each key pathway (n = 4).

(C) Secreted [^{13}C]-labeled lactate concentration in the media of cardiomyocytes (red bar) and ESCs (blue bar) (n = 4). All data were obtained from independent experiments.

*$p < 0.05$; **$p < 0.01$. Data are shown as mean ± SD. All the abbreviations are shown in Table S1. See also Figure S1 and Table S1.

noninvasive environmental approach for their purification from PSC cultures.

RESULTS

Integrated Transcriptomic and Metabolomic Analyses Highlight Distinct Metabolic Differences between Cardiomyocytes and Other Proliferating Cells

To find metabolism-related genes that are differentially expressed between undifferentiated stem cells and cardiomyocytes, we performed comparative transcriptome analyses of undifferentiated mouse ESCs and neonatal mouse cardiomyocytes purified by the "mitochondrial method"(Hattori et al., 2010) (Figures S1A and S1B available online). The results for cardiomyocytes revealed markedly higher expression of genes encoding enzymes involved in the TCA cycle than the undifferentiated ESCs and, in turn, lower expression of genes involved in the pentose phosphate, amino acid synthesis, and lipid synthesis pathways (Figure 1A and Table S1). Next, we conducted a fluxome analysis (Kinoshita et al., 2007; Shintani et al., 2009) to trace a range of metabolites derived from [^{13}C]-labeled glucose in neonatal rat cardiomyocytes, mouse ESCs, a hepatocyte cell line (HepG2), and a skeletal myoblast cell line (C2C12). [^{13}C]-labeled intermediate metabolites of the glycolytic, pentose phosphate, and amino acid synthesis pathways were subsequently found at higher levels in ESCs, HepG2, and C2C12 cells than in cardiomyocytes (Figures 1A, 1B, and S1C and Table S1). ESCs, HepG2, and C2C12 cells also discarded more lactate than cardiomyocytes did (Figure 1C and Figure S1D). In contrast, cardiomyocytes took up pyruvate into mitochondria, and most [^{13}C]-labeled intermediate metabolites of the TCA cycle were significantly higher in cardiomyocytes than in ESCs (Figure 1A). These transcriptome and fluxome analyses highlighted a dynamic difference in the metabolic fates of lactate between cell types (Figure S1E). More specifically, lactate was discarded by noncardiomyocytes but preferentially used in TCA metabolism by cardiomyocytes. We hypothesized that cells mainly dependent on glycolysis might not be able to survive under glucose-depleted and lactate-abundant conditions, whereas cardiomyocytes would survive by using lactate as an alternative energy source.

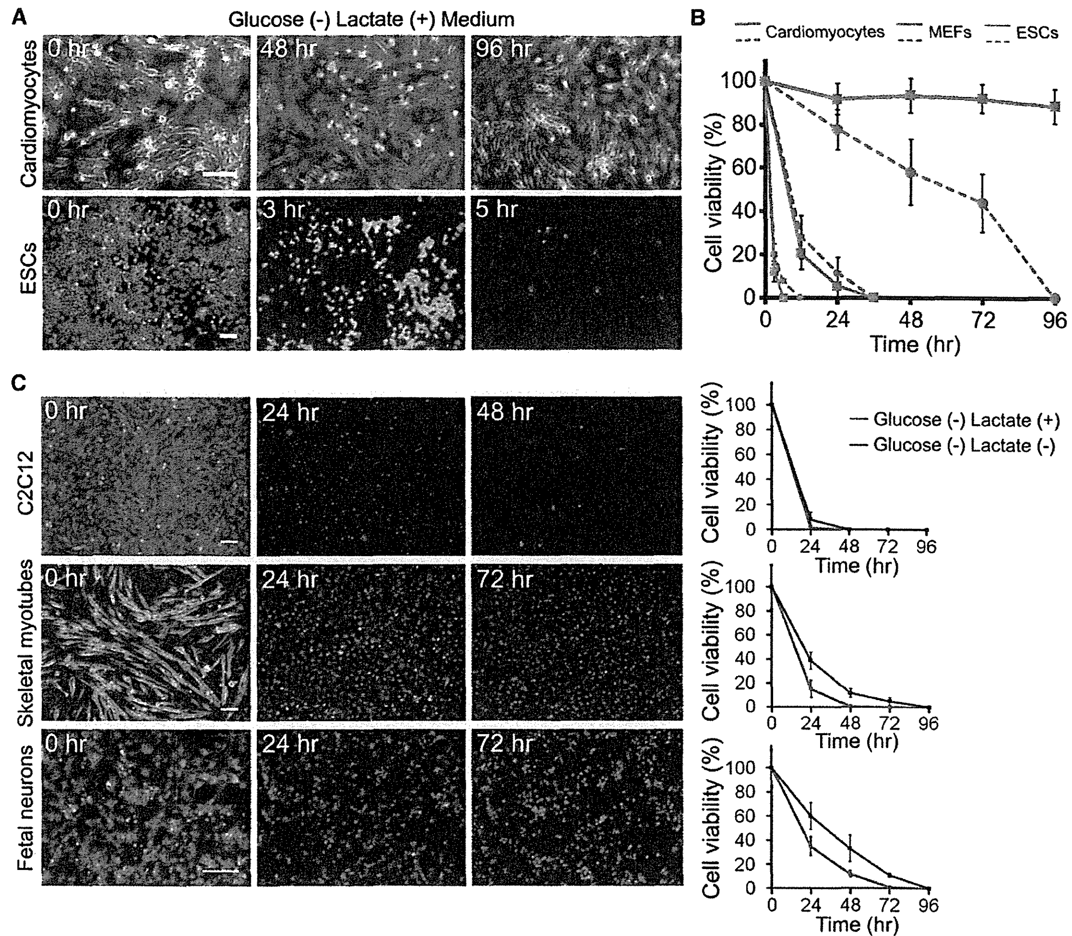

Figure 2. Cell Viabilities of Various Cells under Glucose-Depleted and Lactate-Supplemented Conditions

(A) Cultured neonatal rat cardiomyocytes and mouse ESCs were exposed to glucose-depleted media supplemented with lactate, and their viabilities were assessed with the LIVE/DEAD kit, which indicates viable cells with green fluorescence and dead cells with nuclear red fluorescence.

(B) Time course of viability in neonatal rat cardiomyocytes (red), mouse ESCs (blue), and MEFs (green) under glucose-free conditions with and without lactate (n = 6). Solid lines indicate the glucose-free and lactate-supplemented condition, and dashed lines indicate the glucose-free without lactate condition. All data were obtained from independent experiments.

(C) Noncardiomyocytes including C2C12, skeletal myotubes, and primary cultured neurons were exposed to glucose-free conditions with and without lactate, and their viabilities were assessed with the LIVE/DEAD kit. The time courses of viability were plotted in the line graphs (right) (all cells; n = 4). Red lines indicate the glucose-free and lactate-supplemented condition, and black lines indicate the glucose-free without lactate condition. The inset in primary neurons represents immunocytochemical staining with an antibody to βIII-tubulin (red) and with DAPI (blue).

Scale bars represent 100 μm (A and C). Data are shown as mean ± SD. See also Figure S2.

Glucose-Depleted and Lactate-Enriched Culture Conditions Can Purify Cardiomyocytes from Mouse and Human PSC Derivatives

To test our hypothesis, we exposed neonatal rat cardiomyocytes, mouse ESCs, primary peripheral lymphatic cells, primary fetal neurons, primary mouse embryonic fibroblasts (MEFs), C2C12 cells (myoblasts and myotubes), hepatocytes (HepG2), and renal cells (HEK293) to glucose-depleted conditions with and without various concentrations of lactate. Every type of cell died within 96 hr in the glucose-depleted conditions, and as expected, supplementation with lactate only prolonged the survival of cardiomyocytes (Figures 2A, 2B, 2C and S2). We named this special culture condition for the growth of cardiomyocytes the "lactate method."

We next applied the lactate method to purifying human PSC-derived cardiomyocytes. First, we optimized the time course of the method for human ESC (hESC)-derived cardiomyocytes. Using time-lapse imaging, we observed that 7 days' exposure of hESC- and human iPSC (hiPSC)-derived attached embryoid bodies (EBs) to glucose-free conditions supplemented with 4 mM lactate selectively enriched for beating cells (Movie S1). Second, we confirmed that days 7–8 of culture were the best time points for harvesting the cells, as shown in Figure 3A. To optimize the lactate concentration, we measured the viability

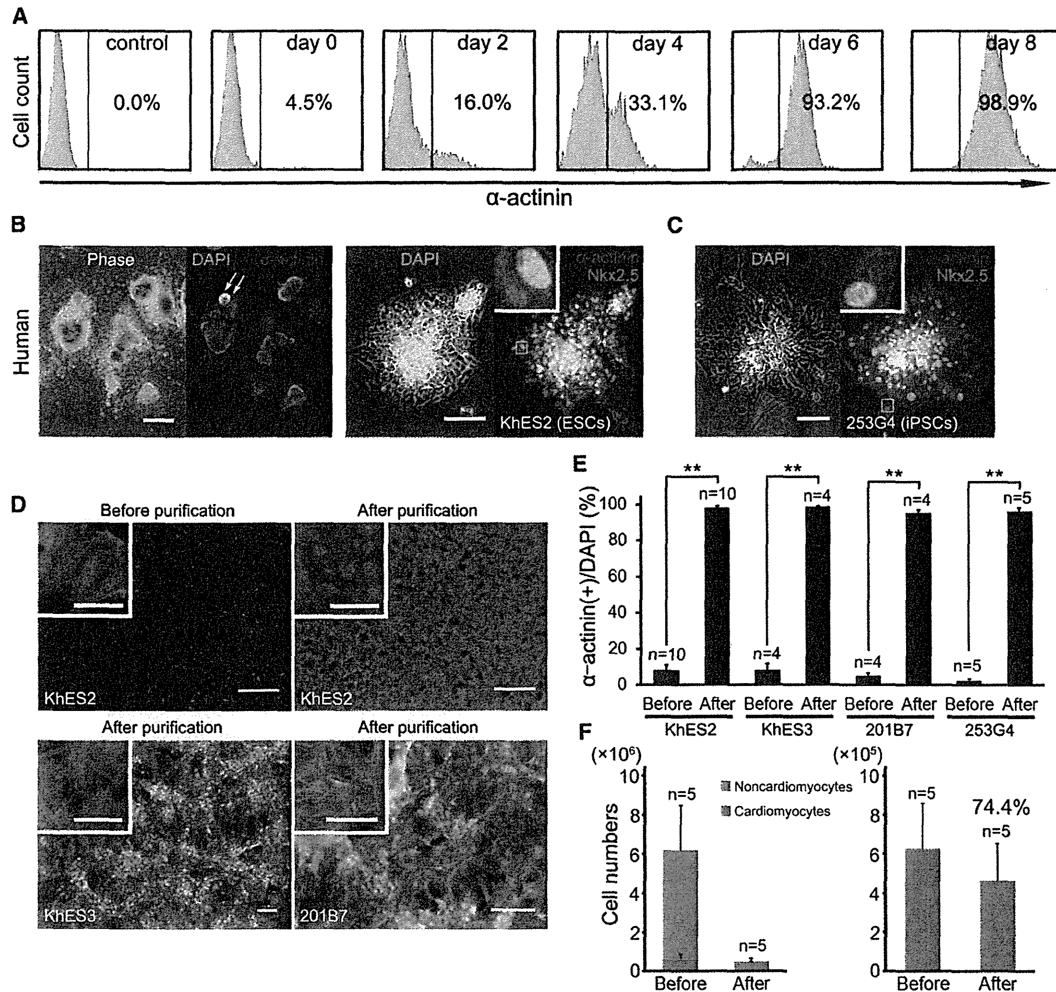

Figure 3. Purification of Cardiomyocytes under Glucose-Depleted and Lactate-Supplemented Conditions

(A) Representative FACS analyses for α-actinin expression in the hESC-derived cells during metabolic selection. Control indicates hESC-derived cells after 2 days of differentiation that do not contain any cardiomyocytes.

(B and C) Representative phase-contrast and immunofluorescent staining for α-actinin in the nonpurified hESC-derived EBs (B, left) and for α-actinin and Nkx2.5 in purified hESC (KhES-2)-derived cardiomyocytes (hESC-CMs) (B, right) and purified hiPSC (253G4)-derived cardiomyocytes (hiPSC-CMs) (C). Arrows indicate α-actinin-positive cells.

(D) Representative immunofluorescent staining for α-actinin (red) in the hESC (KhES-2 and KhES-3)- and hiPSC (201B7)-derived dispersed cells before (upper left) and after (upper right, lower panels) metabolic selection. The cell nuclei are stained by DAPI (blue).

(E) Percentage of α-actinin-positive cardiomyocytes in the hESC (KhES-2 and KhES-3)- and hiPSC (201B7 and 253G4)-derived dispersed cells before and after metabolic selection. All data were obtained from independent experiments.

(F) Numbers of α-actinin-negative noncardiomyocytes (green) and α-actinin-positive cardiomyocytes (red) in the hESC-derived dispersed cells before ($n = 5$) and after ($n = 5$) metabolic selection (left graph). The right graph represents only α-actinin-positive cardiomyocytes. All data were obtained from independent experiments.

Scale bars represent 50 μm (D, insets), 100 μm (B, right; C and D, lower panels), and 500 μm (B, left; D, upper panels). $^{**}p < 0.01$. Data are shown as mean ± SD. See also Figure S3 and Movies S1, S2, and S3.

of purified hESC-derived cardiomyocytes exposed to glucose-depleted conditions with various concentrations of lactate for 6 days; we found the lowest numbers of dead cells in 4 mM lactate (Figure S3A). We further tested for the ideal period of differentiation using the lactate method and found that 20–30 days of differentiation produced the highest reproducibility, purity, and yield of cardiomyocytes. To determine why this period is optimal, we investigated the proliferative activity of EBs on various differentiation days (days 14–60) using a 5-ethynyl-20-deoxyuridine (EdU) incorporation assay. The percentage of EdU-incorporated cells markedly decreased after day 30 (Figure S3B), implying that proliferating cells are sensitive to the lactate method. The optimized condition efficiently enriched for globally contracting aggregates in a time-dependent manner (Figure S3C and Movie S2). Concomitantly, messenger RNA (mRNA) expression of the cardiomyocyte-related gene

Cell PRESS

MYH6 increased, while that of the pluripotency-related gene *POU5F1* (Figure S3D) decreased abruptly. In addition, the mRNAs for noncardiac genes (*NANOG*, *MYOD*, *AFP*, and *MAP2*) were completely eliminated, and those for other cardiomyocyte-related genes (*ACTC1* and *NKX2.5*) were significantly enriched (Figures S3E and S3F). We also observed clumps of purified cardiomyocytes in the adhered condition (Figures 3B and 3C). We dispersed the clumps and cultured the cells therein and then evaluated their purity before and after metabolic selection. The percentages of α-actinin-positive cells before and after metabolic selection were 8.1 ± 2.9% (n = 10) and 98.3 ± 0.9% (n = 10), respectively (Figures 3D and 3E). We also confirmed the efficacy of the lactate method using other hESC (KhES-3) and hiPSC (201B7 and 253G4) lines. As shown in Figures 3D and 3E, the purities were determined as 98.9 ± 0.3, 95.5 ± 1.3, and 96.5 ± 2.0%, respectively. To identify selective events in KhES-2 and iPSCs (253G4 and 201B7), we obtained global gene-expression patterns for the PSC-derived EBs and purified hESC-derived cardiomyocytes. We categorized the expressed genes following the gene ontology consortium and found both similarities and differences among EBs derived from three cell lines (Ashburner et al., 2000). One possible explanation for the differences is that the derived EBs contain various types of cells that are eventually eliminated by the lactate-purification method (Figures S3G and S3H). In our system, 4.0×10^6 hESCs differentiated into $6.2 \pm 2.5 \times 10^6$ (n = 5) cells containing $6.3 \pm 2.3 \times 10^5$ (n = 5) α-actinin-positive cardiomyocytes, and $4.7 \pm 1.8 \times 10^5$ (n = 5) α-actinin-positive cardiomyocytes were finally purified via the lactate method. Therefore, the yield-based efficiency of our lactate method for hESCs was 74.4 ± 12.1% (Figure 3F). To directly compare the yield-based efficiencies between the lactate method and our previous mitochondrial method, we evaluated the yield and found 52.9 ± 12.8% recovery of cardiomyocytes in our previous mitochondrial method (Figure S3I). To determine the types of noncardiomyocyte cells remaining after metabolic selection, we performed immunocytochemical screening and found that most of the cells were smooth muscle actin (SMA)-positive (Figure S3J). Interestingly, α-actinin- and SMA-double-positive cells were also found (data not shown), consistent with a previous report that immature cardiomyocytes express SMA (Clément et al., 2007).

We then applied the lactate method to mouse ESCs using lactate concentrations and timings optimized through similar preliminary experiments for mouse cells. EBs attached to the dishes were exposed to glucose-depleted and 1 mM lactate-supplemented conditions. After 7 days of selection, we recovered the surviving cells by collagenase digestion and transferred them into new fibronectin-coated plates (Movie S3). Immunofluorescence staining revealed that most of the surviving cells were positive for the cardiac markers α-actinin and GATA4 (99.4 ± 0.6% purity, n = 5) (Figure S3K).

Cardiomyocytes Showed High Lactate Uptake and Used Lactate for Metabolic-Energy Production

Why do only cardiomyocytes survive under the lactate-method condition? To address this question, we first compared the [^{14}C]-lactate uptake activity of neonatal rat and human ESC-derived cardiomyocytes, ESCs, MEFs, and noncontracting EBs, and found that both cardiomyocyte populations showed higher levels of activity than the other cells (Figures 4A and 4C). We then measured the changes in intracellular ATP levels in cardiomyocytes and other cells under lactate-method conditions and found that the levels in mouse ESCs, MEFs, and noncontracting EBs fell abruptly, whereas those in neonatal rat and purified human ESC-derived cardiomyocytes were sustained for significantly longer (Figures 4B and 4D). These results indicated that cardiomyocytes, but not noncardiomyocytes, can effectively uptake and use lactate to maintain ATP levels.

Lactate supplementation has the potential to cause acidification either intracellularly or in the medium, which could lead to cellular damage. We therefore investigated whether 4 mM lactate supplementation affects extra- and intracellular pH values. The extracellular pH values were stable at 7.5 following 1 hr of incubation in a 5% CO_2 incubator (Figure S4A). The intracellular pH values of cardiomyocytes, mouse ESCs, MEFs, and C2C12 myoblasts were not affected by supplementation with 4 mM lactate, but all were significantly decreased by the addition of 20 mM lactate (Figures S4B and S4C). Lactate can be transported by monocarboxylic acid transporters (MCTs), of which subtype 1 is abundantly expressed in muscle cells and localizes at both the plasma and mitochondrial inner membrane (Hashimoto et al., 2006). For investigation of the significance of MCT1 expression for lactate uptake in cardiomyocytes, the cells were treated with MCT1 inhibitor α-cyano-4-hydroxycinnamate (α-CHC) (Sonveaux et al., 2008) under glucose-free and lactate-rich conditions. The lactate-induced prolonged survival of cardiomyocytes under glucose-free conditions was largely abolished by the MCT1 inhibitor, despite the lack of α-CHC toxicity, suggesting that lactate uptake via MCT1 plays a major role in the long-term survival of cardiomyocytes under metabolic selection (Figure 4E). To investigate why cardiomyocytes can effectively take up lactate, we checked the expression levels of MCT1 in cardiomyocytes and ESCs but could not find a marked difference between the two (Table S1). We then performed electron microscopy on the hESCs and their derivative cardiomyocytes, as well as mitochondrial staining of hESC-derived cells. The cardiomyocytes showed substantially higher numbers of mitochondria than ESCs and other noncardiomyocytes (Figures S4D and S4E). Because MCTs are passive transporters, we suggest that a major mechanism underlying the enhanced lactate uptake in cardiomyocytes could be the concentration gradients generated by effective lactate consumption via the highly active TCA cycle.

We further investigated how lactate is metabolized in various types of cells. We performed lactate fluxome analysis in mouse ESCs, hESC-derived EBs, MEFs, and neonatal rat cardiomyocytes under glucose-depleted conditions for short (30 min) periods. As expected, high levels of [2,4,5-^{13}C]-citrate, [3,4-^{13}C]-succinate, and [2,3,4-^{13}C]-malate were detected in cardiomyocytes, whereas the ESCs, hESC-derived EBs, and MEFs showed only small amounts of these metabolites, suggesting that exogenous lactate is more efficiently metabolized via the TCA cycle in cardiomyocytes than in noncardiomyocytes, including ESCs (Figure 5 and Figure S5). To our surprise, [^{13}C]-labeled glycolytic intermediates including G6P were observed in both cardiomyocytes and ESCs. These were eventually consumed in the pentose phosphate pathway for production of inosine, guanosine, and adenosine monophosphates.

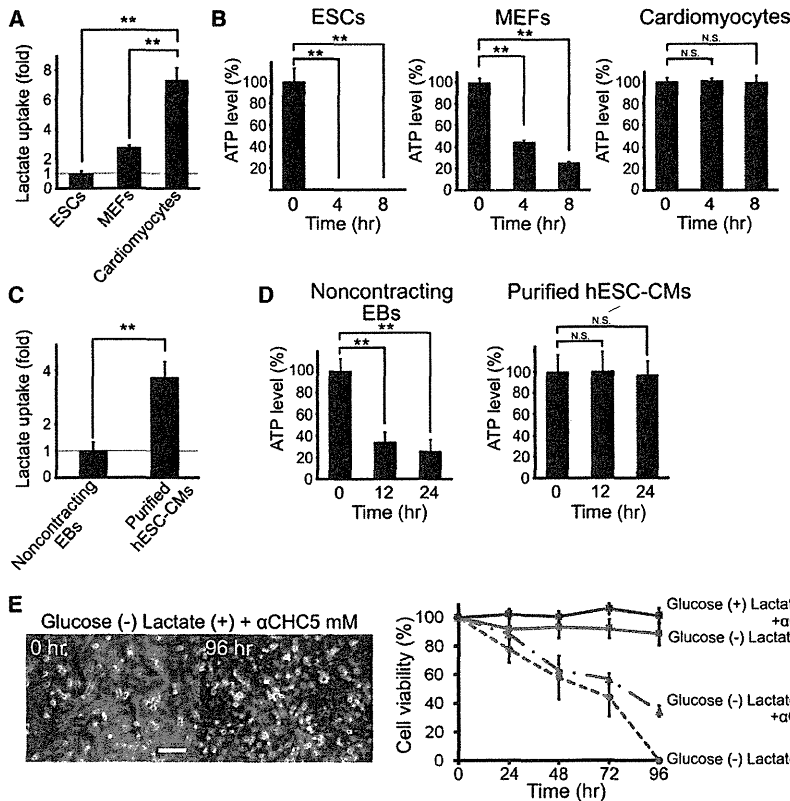

Figure 4. Lactate Uptake and Energetic Homeostasis in Various Types of Cells under Glucose-Depleted and Lactate-Supplemented Conditions

(A and C) [^{14}C]-labeled lactate uptake abilities in (A) mouse ESCs, MEFs, and rat neonatal cardiomyocytes (n = 3) and (C) in noncontracting hESC-derived EBs and purified hESC-CMs (n = 3). All data were obtained from independent experiments.

(B and D) Intracellular ATP levels in (B) the mouse ESCs, MEFs, and neonatal cardiomyocytes (n = 3), and (D) in noncontracting hESC-derived EBs and purified hESC-CMs (n = 3) under glucose-depleted and lactate-supplemented conditions. Relative ATP levels are indicated as percentages of the levels in untreated samples. All data were obtained from independent experiments.

(E) Cultured neonatal rat cardiomyocytes were exposed to glucose-free with lactate conditions supplemented with MCT1 inhibitor (α-CHC, 5 mM), and their viabilities were visualized using the LIVE/DEAD kit (left). The time course of the cardiomyocyte viabilities under different culture conditions is shown (right). Chain and solid red lines indicate glucose-depleted and lactate-supplemented medium supplemented with (n = 4) and without (n = 6) MCT1 inhibitor, respectively. The dashed red line indicates the glucose-depleted without lactate condition (n = 6). The blue solid line indicates high-glucose medium supplemented with MCT1 inhibitor (n = 4). All data were obtained from independent experiments.

Scale bar represents 100 μm (E). *p < 0.05; **p < 0.01. Data are shown as mean ± SD. See also Figure S4.

Long-period (24 hr) fluxome analysis in viable cardiomyocytes also detected [5-^{13}C]-labeled reduced (GSH) and [4,5,6,7,8,10-^{13}C]-labeled oxidized glutathione (GSSG), indicating that glutamate, glycine, and/or cysteine were also synthesized from the lactate (Figure 5 and Table S2).

Purified hESC-Derived Cardiomyocytes Showed High Proliferative Capacity

We next investigated the proliferative capacity of mouse and human ESC-derived cardiomyocytes purified using metabolic selection. Some of the purified cardiomyocytes expressed Ki67 antigen (Figure 6A) and showed EdU-incorporation activities (Figure 6B). For directly assessing the rate of karyokinesis and cytokinesis after metabolic selection, the purified hESC-derived aggregates were completely dissociated and then seeded sparsely onto the MEF-layered dishes. Counting of immunocytochemically α-actinin-positive cells after 2, 4, 6, and 8 days revealed that the purified cardiomyocytes could proliferate up to 2.5-fold in 8 days, and the fraction of multinuclear cardiomyocytes increased over time compared with the second day (Figure 6C).

Purified Human PSC-derived Cardiomyocytes Showed Physiologically Relevant Action-Potential Configurations and Drug Responses

Action-potential recording using glass microelectrodes revealed that the purified hESC-derived cardiomyocytes had nodal- (14 of 76), atrial- (23 of 76), or ventricular-like (39 of 76) action potentials (Figure 6D and Figure S6A). We next evaluated their chronotropic response to the β-agonist isoproterenol and muscarinic agonist carbamylcholine using the multielectrode array (MEA) system; the former agent increased the beating frequency, whereas the latter decreased it, both in a dose-dependent manner (Figure 6E). We also found that beat frequency could be modulated by temperature (Figure S6B), and intracellular [Ca^{2+}] recording using Fluo-4 dye also revealed that the purified hESC-derived cardiomyocytes showed spontaneous and synchronized Ca^{2+} oscillations (Figure S6C).

Transplanted Purified Cardiomyocytes Did Not Form Tumors

Finally, for investigation of the potential tumorigenicity of the purified cardiomyocyte populations, 1,000 undifferentiated hESCs, 2.0 × 10^5 nonpurified hESC-derived cardiomyocytes, or the same number of purified cells were transplanted into the testes of immunocompromised nonobese diabetic severe combined immunodeficient (NOD-SCID) mice. Two months later, 9 of 10 (90%), 8 of 20 (40%), and 0 of 20 mice developed tumors, respectively (Figure 6F and Figure S6D). For further verification of the absence of residual undifferentiated cells, nonpurified and purified dispersed hESC-derived cells (2.0 × 10^5) were cultured on MEFs under PSC maintenance culture conditions (colony formation assay) for 4 days. Nonpurified hESC-derived cells formed Oct3/4- or Tra1-60-positive piled-up colonies, but

Cell PRESS

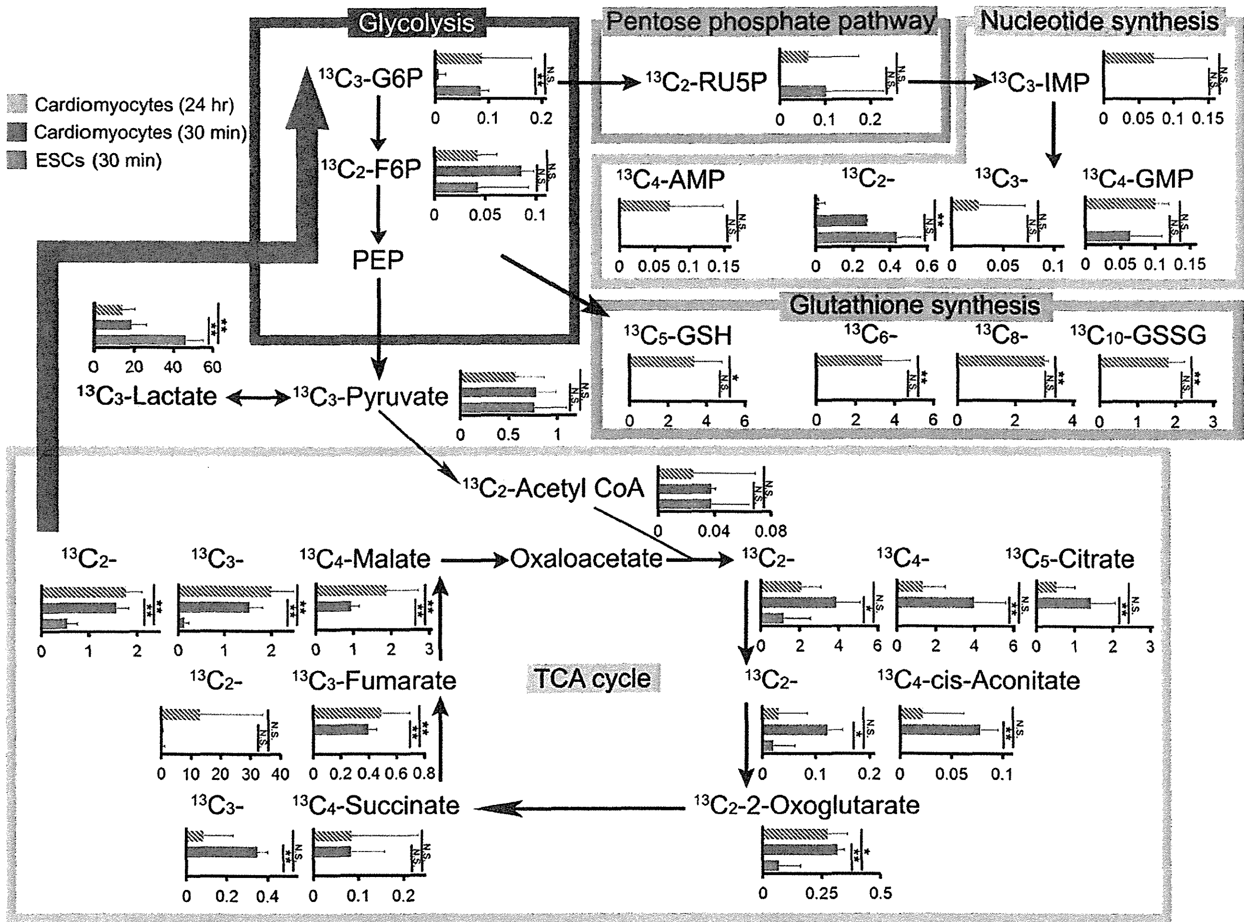

Figure 5. Mechanisms Underlying the Lactate-Mediated Survival of Cardiomyocytes

Fluxome analysis of the short-term (30 min) and long-term (24 hr) administration of [^{13}C]-labeled lactate under glucose-depleted conditions in neonatal cardiomyocytes and ESCs (ESCs, n = 4; cardiomyocytes, n = 3). The relationships between the kinds of bars, kinds of cell, and labeling conditions are shown in the upper left. All data were obtained from independent experiments. The bold red arrow on the right indicates a possible reflux pathway from malate to G6P. All units are nmol per 1.0 × 10^7 cells. *$p < 0.05$; **$p < 0.01$. Data are shown as mean ± SD. PEP, phosphoenolpyruvate. See also Figure S5 and Table S2.

the purified cardiomyocytes formed no colonies (Figure 6G and Figure S6E). To demonstrate the PSC-elimination capacity of the lactate method, we used a commercially available kit based on magnetic-beads-activated cell sorting with a Tra1-60 antibody. This experiment confirmed the apparent superiority of the lactate method in eliminating stem cells compared to the tested method (Figure S6F).

DISCUSSION

There are several approaches available for obtaining enriched cardiomyocyte populations from human PSCs. Ma et al. (2011) performed genetic-modification-based purification of cardiomyocytes (achieving >98% cardiomyocyte purity) from hiPSC derivatives, using the intrinsic *MYH6* gene to express a blasticidin S resistance gene. Dubois et al. (2011) used a surface protein, signal-regulatory protein alpha (SIRPA), as a cardiac-specific marker in hiPSC derivatives prepared through a highly cardiogenic differentiation procedure. They purified cardiomyocytes (up to 98% purity) via FACS from sources comprising 40%–50% cardiomyocytes. The method we report here is a simple medium-exchanging procedure that enabled cardiomyocyte purification of up to 99% from a cell source comprising only 10% cardiomyocytes, with an estimated recovery of cardiomyocytes of 74.4 ± 12.1%, based on direct cell count before and after purification. Previously we reported a mitochondrial method for purifying cardiomyocytes to >99% purity via FACS. Our direct comparison of these two methods revealed a higher cardiomyocyte-yield-based efficiency for the lactate method than for the mitochondrial method. The lactate method has quantitative and economic advantages relative to other existing cardiomyocyte-purification methods by virtue of its simplicity and ease of application.

One question that arose from our studies is why ESCs die within a few hours under the lactate method but cardiomyocytes survive for much longer, even though both cell types use lactate

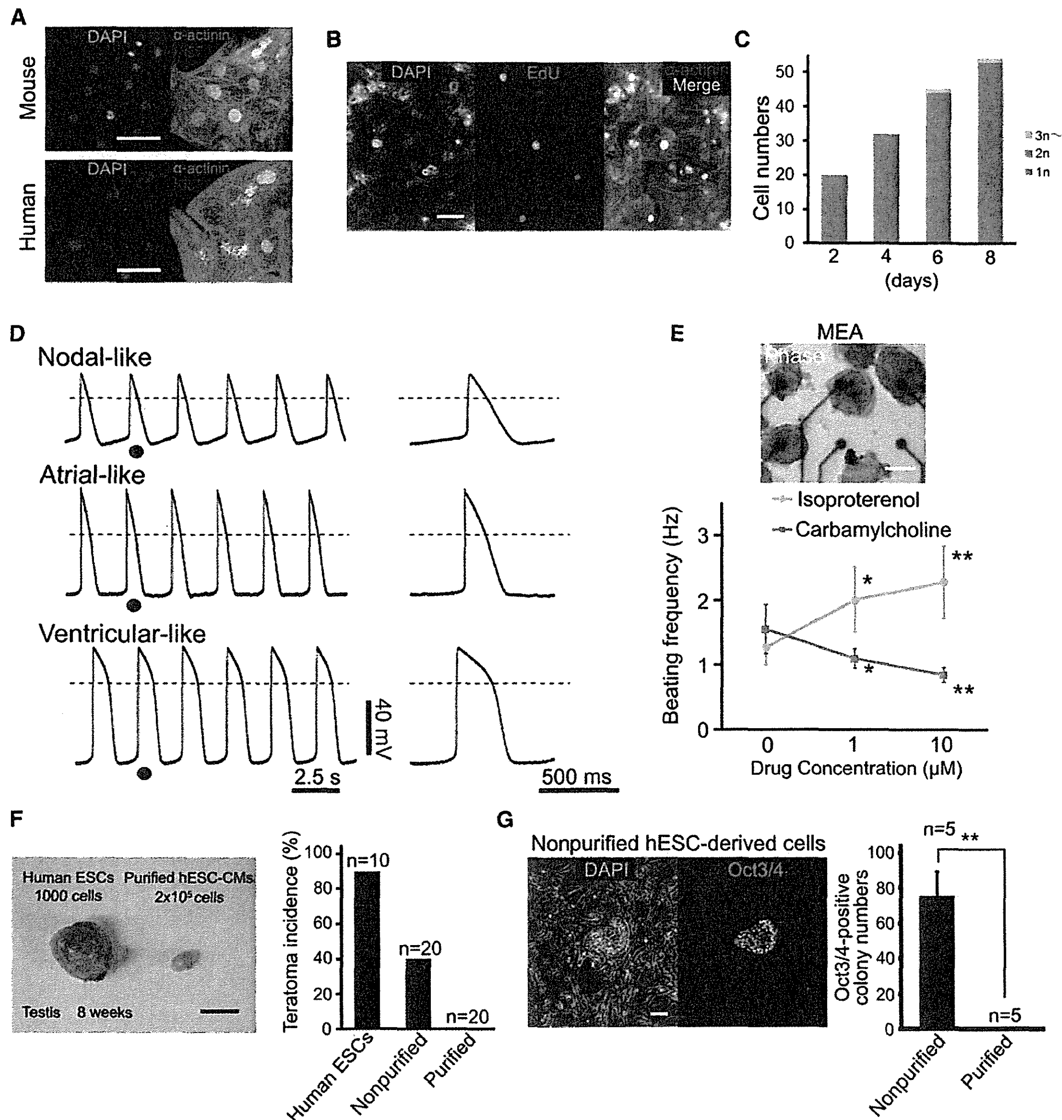

Figure 6. Characterization of ESC-Derived Cardiomyocytes after Metabolic Selection

(A) Immunofluorescent staining for α-actinin (green) and Ki67 (red) in the purified mouse (top) and human (bottom) ESC-CMs.

(B) EdU-positive cells (green) in purified hESC-CMs.

(C) Numbers of hESC-derived dispersed cardiomyocytes after metabolic selection. The numbers of cardiomyocytes with single, double, and more than triple nuclei are separately represented by the blue, red, and green bars, respectively.

(D) Action-potential recording of the purified hESC-CMs using microelectrodes. Shown are representative configurations of the nodal- (top), atrial- (middle), and ventricular-like (bottom) action potentials.

(E) Drug responses in purified hESC-derived aggregates using the MEA system (top). The line graph (bottom) represents the chronotropic response against β-agonist isoproterenol (green; n = 3) and muscarinic agonist carbamylcholine (orange; n = 3). All data were obtained from independent experiments.

(F) The teratoma-forming capacities of hESCs (1,000 cells), nonpurified hESC-derived cells (2.0×10^5 cells), and purified hESC-CMs (2.0×10^5 cells) were evaluated through their transplantation into the testes of NOD-SCID mice. The bar graph represents the summarized results (hESCs, n = 10; nonpurified, n = 20; purified, n = 20).

(G) Immunofluorescent staining for Oct3/4 in dispersed cells from nonpurified hESC-derived EBs. The bar graph shows numbers of hESC-like colonies obtained from hESC-derived cells (2.0×10^5; n = 5).

Scale bars represent 50 μm (A and B), 100 μm (E and G), and 1 cm (F). *$p < 0.05$; **$p < 0.01$. Data are shown as mean ± SD. See also Figure S6.

for biomass synthesis. Through our investigations, we eliminated the possibility that lactate supplementation caused toxic extracellular or intracellular acidification. We propose that these differing properties may be a result of (1) the retrospective glycolytic pathway consuming two ATP molecules during conversion of a lactate molecule to G6P, and (2) ESCs not being

Cell PRESS

able to effectively obtain ATP from glycolysis nor from OXPHOS under glucose-depleted conditions. Therefore, activation of the retrospective glycolytic pathway may accelerate a catastrophic balance of ATP supply and demand in ESCs, whereas cardiomyocytes can maintain cellular ATP homeostasis by producing more ATP via a highly active OXPHOS mechanism (Hattori et al., 2010).

A patient would theoretically require about 10^9 cardiomyocytes in therapeutic applications of purified cardiomyocytes. In this study, we obtained approximately 5×10^5 purified human cardiomyocytes per 177 cm^2 dish. Taking into account their postpurification proliferative capacities, rough estimates therefore suggest that 1×10^9 cardiomyocytes could be obtained from 800 dishes (14.13 m^2). This scale is close to the capacity of commercially available automatic large-scale culture systems and suggests that combining more sophisticated differentiation methods with our lactate method could facilitate realistic application of PSC-derived cardiomyocytes to human therapy.

EXPERIMENTAL PROCEDURES

Animals

All animals including pregnant ICR mice, neonatal Wistar rats, and NOD-SCID mice (8 weeks old, male) were purchased from CLEA Japan (Tokyo). All experimental procedures and protocols were approved by the Animal Care and Use Committee of Keio University and conformed to the National Institutes of Health Guide for the Care and Use of Laboratory Animals.

Cells

Mouse ESCs were obtained from the Laboratory of Pluripotent Cell Studies, RIKEN Center for Developmental Biology. The hESC line (KhES-2 and KhES-3) was obtained from the Department of Development and Differentiation, Institute for Frontier Medical Sciences, Kyoto University and used in conformity with the Guidelines for Derivation and Utilization of Human Embryonic Stem Cells of the Ministry of Education, Culture, Sports, Science, and Technology, Japan. The hiPSC line (253G4 and 201B7) was obtained from the Center for iPSC Research and Application, Kyoto University. The skeletal myoblast cell line (C2C12), hepatocyte cell line (HepG2), and renal cell line (HEK293) were obtained from the American Type Culture Collection.

Reagents

The mouse monoclonal antibodies for α-actinin (immunoglobulin G_1 [IgG_1]) and Ki67 (IgM) were purchased from Sigma-Aldrich (Sigma). The mouse monoclonal antibodies for SMA (IgG_{2a}), βIII-tubulin, Oct3/4, and Tra1-60 were purchased from Dako, Promega, BD Transduction Laboratories, and Millipore, respectively. The goat polyclonal antibodies for GATA-4 (C-20) and Nkx2.5 (N-19) were purchased from Santa Cruz Biotechnology (Santa Cruz). Alexa Fluor 488 and 546 anti-mouse IgG (IgG_1, IgG_{2a}, and IgM) antibody and anti-goat IgG antibody were purchased from Invitrogen. DAPI and E-cadherin-Fc were also purchased from Invitrogen. Tetramethylrhodamine methyl ester perchlorate (TMRM), mitotracker red, 2′,7′-bis-(2-carboxyethyl)-5-(and-6)-carboxyfluorescein (BCECF) and Fluo-4 dye were purchased from Invitrogen. Fibronectin, isoproterenol hydrochloride, carbamylcholine, and α-CHC were purchased from Sigma. The [^{13}C]-labeled glucose and lactate were purchased from Isotec. The [^{14}C]-labeled lactate was purchased from PerkinElmer.

Maintenance of Mouse and Human PSCs

We maintained mouse ESCs on gelatin- or E-cadherin-coated dishes in Glasgow minimum essential medium (MEM) (Sigma) supplemented with 10% fetal bovine serum (FBS; Equitech-Bio), 0.1 mM MEM nonessential amino acid solution (Sigma), 2 mM L glutamine (Sigma), 0.1 mM β-mercaptoethanol (Sigma), and 2,000 U/ml murine leukemia inhibitory factor (Chemicon) (Nagaoka et al., 2006). We maintained hESCs and hiPSCs on MEFs in Dulbecco's modified Eagle's medium/nutrient mixture F-12 Ham 1:1 (DMEM-F12; Sigma) supplemented with 20% knockout serum replacement (Invitrogen), 0.1 mM MEM nonessential amino acid solution (Sigma), 2 mM L glutamine (Sigma), 0.1 mM β-mercaptoethanol (Sigma), and 4 ng/ml basic fibroblast growth factor (Wako).

Differentiation of Human PSC-Derived Cardiomyocytes

We cultured the enzymatically detached undifferentiated colonies of hESCs and hiPSCs with αMEM (Wako Pure Chemical, Wako) that contained 50 μg/ml ascorbic acid, supplemented with 5% FBS (Biowest) and 0.1 mM β-mercaptoethanol in bacterial Petri dishes for formation of EBs. EBs containing rhythmically beating cells were observed 14 to 20 days later. Typically, 1%–10% of EBs contained beating cells. Media were changed once a week. EBs were used for purification experiments between days 20 and 30.

Purification of hESC- and hiPSC-Derived Cardiomyocytes

The selection medium was prepared before use. Glucose-free DMEM (no glucose, no pyruvate; Invitrogen) supplemented with 4 mM lactate medium was produced using 1 M lactate stock solution prepared from diluting 10 M lactate (Wako Pure Chemical) with sterile 1M Na-HEPES (Sigma). The human PSC-derived EBs at differentiation day 20 to 30 were extensively washed with and exposed to the selection medium. Media were changed every 2 or 3 days for eliminating dead cells via rapid flushing using 40 μm filters (Becton Dickinson). Cells were sampled daily from day 6 of purification for optimizing the timing of harvest for each batch. We split sampled cells into two experiments: one for test cultivation and another for FACS analysis. In the test cultivation, cells were transferred to fibronectin-coated dishes and cultured for several days with αMEM supplemented with 5% FBS. FACS analysis was performed using α-actinin antibodies. Our criterion for determining the harvest day was at least 95% purity indicated by FACS analysis. All harvested cells were then transferred to fibronectin-coated dishes and cultured for several more days under αMEM supplemented with 5% FBS, during which the media were changed several times for complete removal of debris consisting of dead cells and insoluble matrix. The purified cardiomyocytes were finally collected by rapid flushing. Movies were recorded using a fluorescence microscope (BZ-9000; Keyence).

Cardiomyocyte Purification Using Mitochondrial Dye for Gene Array

To prepare purified cardiomyocytes for the gene array, we used hearts from neonatal mice (P1). Purification of mouse neonatal cardiomyocytes using mitochondrial TMRM dye was performed by FACS (FACS Aria; Becton Dickinson), as described previously (Hattori et al., 2010).

Immunofluorescence

We fixed cells with 4% paraformaldehyde in PBS (pH 7.0) for 20 min. Subsequently, cells were permeabilized with 0.1% Triton X-100 (Sigma) at room temperature for 10 min and then incubated with the primary antibody at 4°C overnight. Cells were then washed with Tris-buffered saline (TBS) containing 0.1% Tween 20 four times prior to incubation with the secondary antibodies at room temperature for 1 hr. After nuclear staining with DAPI (Invitrogen), stained cells were detected by fluorescence microscopy (IX71; Olympus) or confocal-laser microscopy (LSM 5 DUO; Carl Zeiss).

Cell Viability under Glucose-Depleted Conditions with or without Lactate

Neonatal cardiomyocytes, ESCs, and noncardiomyocytes including MEFs, HepG2, HEK293, peripheral lymphatic cells, C2C12, skeletal myotubes, and fetal neurons were exposed to glucose-free DMEM (Invitrogen) supplemented with or without lactate (Wako). Cell viabilities were determined by the LIVE/DEAD Viability/Cytotoxicity Assay Kit (Invitrogen) based on the simultaneous determination of live and dead cells with the calcein AM and ethidium homodimer-1 probes. Fluorescence imaging of the cells (live cells were labeled green, whereas the nuclei of dead cells were labeled red) was performed with fluorescence microscopy (IX70 microscope; Olympus) equipped with a color charge-coupled device camera (CS220; Olympus). The green-labeled live area was measured using Image J. Relative cell viabilities were calculated in percentages, compared with those before treatment.